The Late Paleozoic Ice Age: An Evolving Paradigm

Isabel P. Montañez[1] and Christopher J. Poulsen[2]

[1]Department of Earth and Planetary Sciences, University of California, Davis, California 95616; email: ipmontanez@ucdavis.edu

[2]Department of Earth and Environmental Sciences, University of Michigan, Ann Arbor, Michigan 48109; email: poulsen@umich.edu

Annu. Rev. Earth Planet. Sci. 2013. 41:629–56

First published online as a Review in Advance on April 3, 2013

The *Annual Review of Earth and Planetary Sciences* is online at earth.annualreviews.org

This article's doi:
10.1146/annurev.earth.031208.100118

Keywords

glacial state, icehouse, greenhouse, Permian, Pennsylvanian, glacioeustasy, CO_2 climate forcing

Abstract

The late Paleozoic icehouse was the longest-lived ice age of the Phanerozoic, and its demise constitutes the only recorded turnover to a greenhouse state. This review summarizes evidence for the timing, extent, and behavior of continental ice on Pangea in addition to the climate and ecosystem response to repeated transitions between glacial and interglacial conditions. Combined empirical and climate modeling studies argue for a dynamic ice age characterized by discrete periods of glaciation separated by periods of ice contraction during intermittent warmings, moderate-size ice sheets emanating from multiple ice centers throughout southern Gondwana, possible glaciation of the Northern Hemisphere, and atmospheric CO_2 as a primary driver of both ice sheet and climate variability. The glacioeustatic response to fluctuations of these smaller ice sheets was likely less extreme than previously suggested. Modeling studies, stratigraphic relationships, and changes in both the geographic patterns and community compositions of marine fauna and terrestrial flora indicate the potential for strong responses to high-latitude glacial conditions in both ocean circulation and low-latitude climate. The forcings and feedbacks of these linkages, as well as existing climate paradoxes, define research targets for future studies of the late Paleozoic.

INTRODUCTION

Although icehouse periods make up less than 25% of the past billion years of Earth's history (Montañez et al. 2011), glacial conditions persisted for ∼70 Ma of the late Paleozoic (Veevers & Powell 1987). The late Paleozoic ice age (herein referred to as the LPIA) was a time of unique convergence of major landscape changes driven by supercontinental reconfiguration (**Figure 1**), the lowest atmospheric levels of CO_2 and the highest levels of O_2 of the Phanerozoic (Berner 2006), and the evolution and expansion of the oldest paleotropical rainforests (Cleal & Thomas 2005). The demise of the icehouse is our only record of a vegetated world transition from a glacial state to fully greenhouse conditions (Gastaldo et al. 1996, Montañez et al. 2007).

The LPIA has long been argued as an analog for the Quaternary glacial state in which humans evolved and live (see, e.g., Raymond & Metz 2004). Early estimates of the LPIA suggested a single, prolonged ice age (**Figure 1*b***) with glacial extents and orbitally paced changes in ice volume and glacioeustasy comparable with those of the Pleistocene (Crowley & Baum 1991). Studies

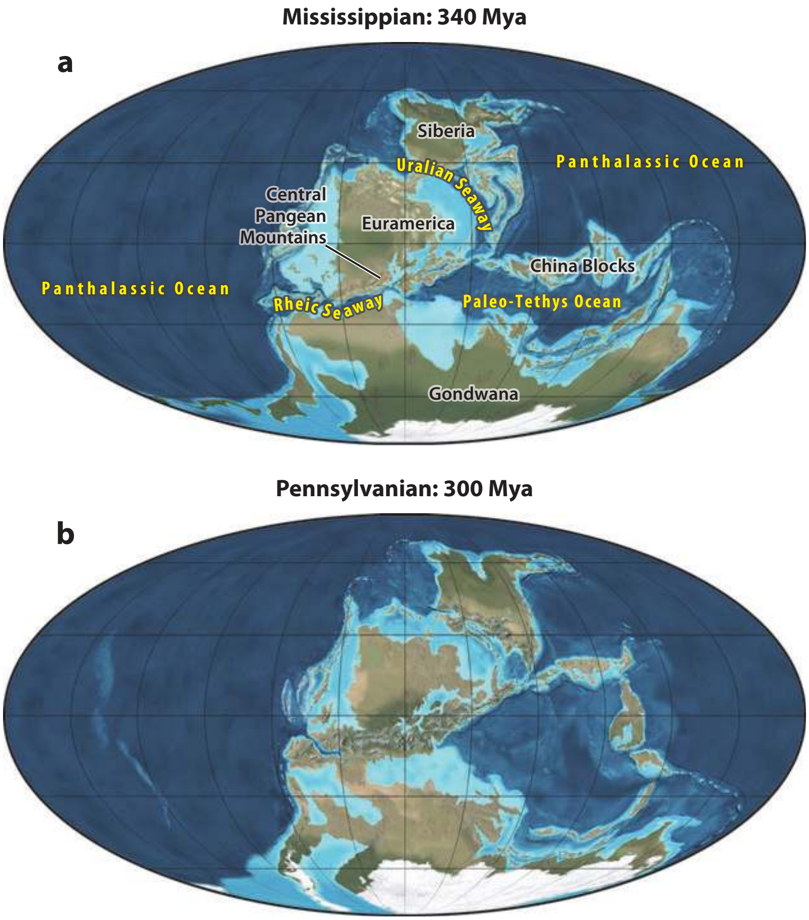

Figure 1

Mollweide paleogeographic maps of (*a*) the Late Mississippian (340 Mya) early icehouse and (*b*) the Early Pennsylvanian (300 Mya) peak icehouse, courtesy of R. Blakey (**http://www2.nau.edu/rcb7/**). Modified to illustrate specific geographic elements such as the major ocean basins and continental landmasses at the time.

of the LPIA over the past two decades paint a more dynamic view characterized by repeated, short-lived, and possibly severe glacial events separated by substantially diminished or ice-free conditions (Isbell et al. 2003, 2012; Fielding et al. 2008a,d). Building on decades of prior research, other studies provide insight into the complex responses of sea level, atmospheric and oceanic circulation, and lower-latitude climate to the waxing and waning of glacial ice and likely variation in atmospheric CO_2 (e.g., Montañez et al. 2007, Poulsen et al. 2007, M.J. Soreghan et al. 2008, Birgenheier et al. 2010, Eros et al. 2012b). Similarly, paleobiologic studies reveal a far less stable biosphere than previously believed, one characterized by major floral and faunal restructuring that accompanied and, in some cases, influenced climate change (Powell 2007, Clapham & James 2008, DiMichele et al. 2009, McGhee et al. 2012).

These recent studies demonstrate the evolution and interaction of components of the climate system and biosphere during the late Paleozoic and suggest the possibility of climate behavior outside the typical range of the Cenozoic glacial state. They also discuss fundamental questions and climate paradoxes, which, along with the research opportunities they present, are the focus of this review.

Cyclothems: fluviodeltaic and marine depositional facies bounded stratigraphically by channelized erosion features and fossil soils; facies exhibit systematic vertical patterns (meters to tens of meters in scale) that record changes in relative sea level

THE ANATOMY OF AN ICEHOUSE

Our evolving understanding of the LPIA in large part reflects the increasing precision of Permo-Carboniferous chronostratigraphy, which permits the regional-to-global correlation of high-resolution stratigraphic, paleobiologic, geochemical, and tectonic records. Early reconstructions proposed a long-lived, expansive ice sheet in southern Gondwana, the extent of which was delineated by encircling the geographic distribution of Gondwanan glacigenic deposits (**Figure 2**). However, this approach does not account for differences in the ages or paleoaltitudes of glacigenic deposits, among other factors (Isbell et al. 2012). Extensive glacially derived loess deposits (Soreghan et al. 2002) and the ubiquity of cyclothems throughout the Pangean paleotropics (see, e.g., Heckel 1977, 1994; West et al. 1997) have long been argued as further evidence for protracted massive ice sheets during the LPIA (which occurred from ~335 to 260 Mya). In turn, glacioeustatic fluctuations (of tens of meters to a hundred meters or more) driven by the orbital-scale (10^5-year) waxing and waning of this large ice sheet(s) have been inferred from cyclothems (see, e.g., Wanless & Shepard 1936, Heckel 1986). Although extensive glaciation in the northern paleo–high latitudes is generally refuted, the presence of dropstones, glaciomarine deposits, and diamictites in Siberia indicates minimal sea or shore ice, or possibly icebergs, at various times during the LPIA (**Figure 2**) (Raymond & Metz 2004, Fielding et al. 2008d).

Multiple independent lines of evidence support a dynamic LPIA—one consisting of a series of discrete (<1 Ma to ~8 Ma) and possibly asynchronous glaciations emanating from numerous ice centers (**Figure 2**) (Visser 1997; Isbell et al. 2003; Fielding et al. 2008a,c; Gulbranson et al. 2010). Notably, periods between discrete glacial events likely had greatly reduced ice volume, providing an archive of repeated deglaciation. In the following subsections, we review the evolution of the LPIA paradigm by drawing on an extensive literature from a broad range of disciplines. **Supplemental Appendix A** (follow the **Supplemental Materials link** from the Annual Reviews home page at **http://www.annualreviews.org**) provides a compilation, by category, of additional relevant references not cited here due to space limitations.

Supplemental Material

Initiation of the LPIA

The earliest indications of Gondwanan glaciation are short-lived events in the latest Devonian and Early Mississippian inferred from glacial deposits in Bolivia (Isaacson et al. 2008), Peru and

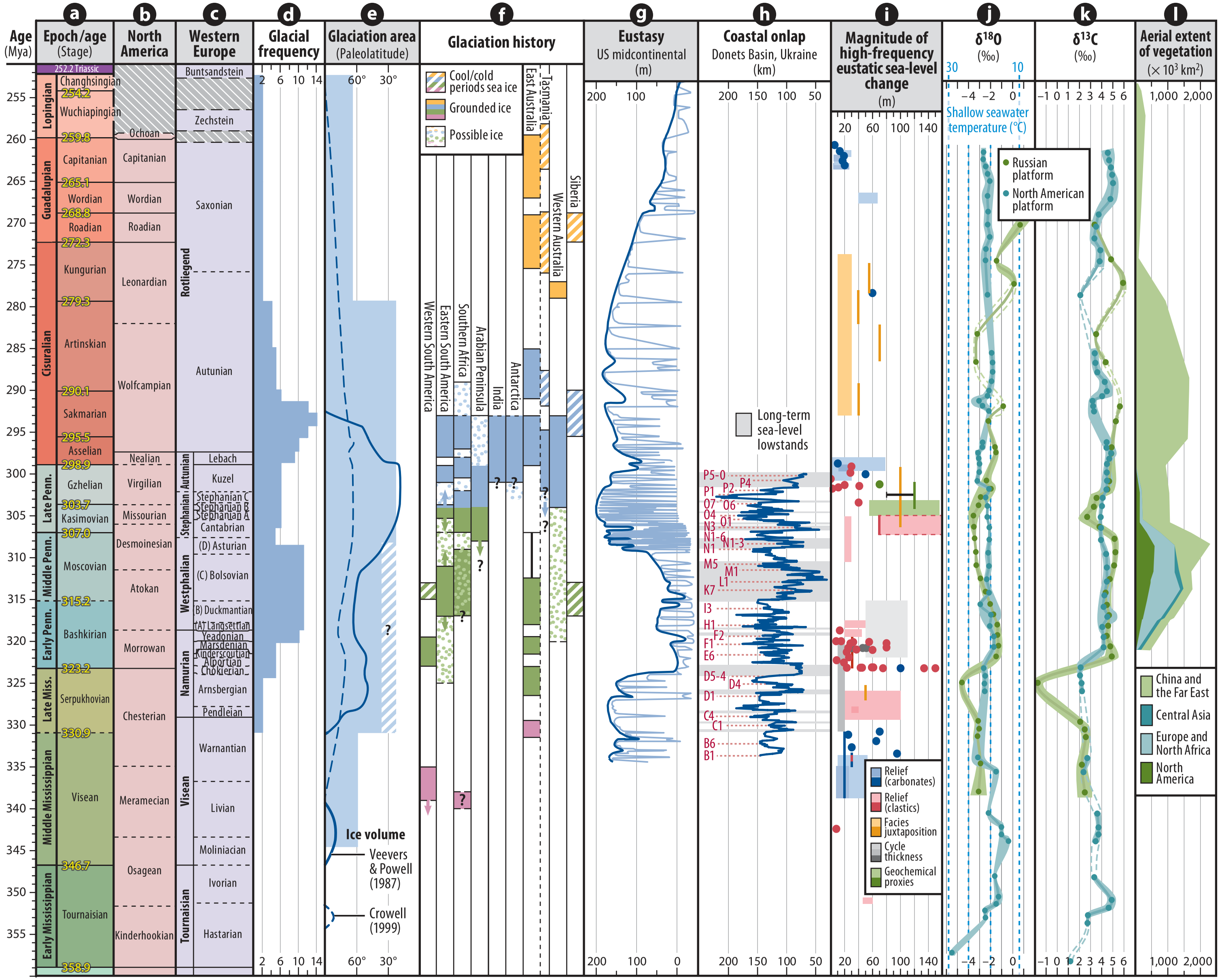
a Epoch/age (Stage)
b North America
c Western Europe
d Glacial frequency
e Glaciation area (Paleolatitude)
f Glaciation history
g Eustasy US midcontinental (m)
h Coastal onlap Donets Basin, Ukraine (km)
i Magnitude of high-frequency eustatic sea-level change (m)
j δ18O (‰)
k δ13C (‰)
l Aerial extent of vegetation (× 10³ km²)
Age (Mya)
Ice volume
Veevers & Powell (1987)
Crowell (1999)
Cool/cold periods sea ice
Grounded ice
Possible ice
Long-term sea-level lowstands
Shallow seawater temperature (°C)
Russian platform
North American platform
Relief (carbonates)
Relief (clastics)
Facies juxtaposition
Cycle thickness
Geochemical proxies
China and the Far East
Central Asia
Europe and North Africa
North America

MARINE CARBONATES AS PROXIES OF SEAWATER CONDITIONS

The carbon and oxygen isotopic compositions of marine fossils composed of low-Mg calcite are considered robust proxies of the conditions under which they formed, if the shells are well screened for evidence of postdepositional diagenetic alteration. Marine fossil carbon isotopes ($\delta^{13}C$ values) are indicators of changes in global C cycling, including changes in the burial and sequestration of organic matter, marine and terrestrial primary productivity, and volcanism. Marine fossil oxygen isotopes ($\delta^{18}O$ values) are proxies of ambient seawater temperature and seawater $\delta^{18}O$ composition. Seawater $\delta^{18}O$ is influenced both by changes in ice volume ($\delta^{18}O$ composition increases as ice accumulates) and by local hydrographic, hydrochemical, and climate conditions that influence seawater salinity. Temperature affects the magnitude of fractionation between seawater and minerals.

Brazil (Caputo et al. 2008), and the Appalachian Basin (Brezinski et al. 2008). Initial glaciation is considered to have been alpine (Isbell et al. 2003), although contemporaneous erosive valleys (~60 m of incision) in tropical successions (Kammer & Matchen 2008) and a positive shift in marine fossil $\delta^{18}O$ values (**Figure 2**) at the Kinderhookian-Osagean boundary suggest that this time period may have been a period of extensive ice volume. A positive shift in marine fossil $\delta^{13}C$ values of $\geq$4‰ suggests a coincident increase in organic C sequestration and a likely drop in atmospheric $p\mathrm{CO}_2$ (Saltzman 2002) (see sidebar, Marine Carbonates as Proxies of Seawater Conditions).

By the Middle to Late Mississippian (mid-to-late Visean to early Serpukhovian), glaciation developed in peripolar circle regions of southern Gondwana (**Figures 2** and **3**) (González 2001, Limarino et al. 2006, Gulbranson et al. 2010, Pérez Loinaze et al. 2010). Coeval low-latitude cyclothems and stacked incised valleys indicate eustatic fluctuations of 20 to 50 m and moderate ice accumulation (**Figure 2**) (Bishop et al. 2009, Waters & Condon 2012). A dynamic climate during the later part of the Mississippian is suggested by (*a*) repeated short-term intercalation of warm-climate floras with more typical cooler-climate (Gondwanan) floral communities (Iannuzzi & Pfefferkorn 2002), (*b*) stepwise superposition of fluctuations aged ~1 ± 0.2 Ma on the relatively stable longer-term sea level (Eros et al. 2012b), and (*c*) possible large fluctuations in tropical shallow-water temperatures, inferred from brachiopod $\delta^{18}O$ compositions (Giles 2012) and Mg/Ca ratios (Powell et al. 2009). The impact of this first phase of glaciation on marine

Figure 2

Summary diagram illustrating the evolution in models of glaciation history and comparisons with other Earth system changes during the late Paleozoic ice age. (*a–c*) Timescale from Davydov et al. (2012) and Henderson et al. (2012). (*d*) Glacial frequency adapted from Frakes et al. (1992) and (*e*) area of glaciation adapted from Frakes & Francis (1988) and Crowley & Baum (1992). (*f*) Glaciation history: Colored bars denote the distribution of glaciation and cool/cold intervals based on data published in reviews by Isbell et al. (2003, 2012), papers in Fielding et al. (2008c), and additional citations in the section Anatomy of an Icehouse. Glacial phases are color coded as follows: Late Mississippian (*pink*), mid-Carboniferous (*green*), latest Carboniferous–early Permian (*blue*), and late early-middle Permian (*orange*). Extent of uncertainty regarding the onset and termination of glaciations is shown by dashed lines, arrows, and question marks (the latter indicate very poorly constrained values). (*g*) Midcontinental eustatic curve adapted from Ross & Ross (1987) and correlated biostratigraphically to (*h*) the Donets coastal onlap curve (Eros et al. 2012a). (*i*) Magnitudes of eccentricity-scale eustasy inferred from the stratigraphic record (modified from Rygel et al. 2008 to remove model-based estimates). (*j*) Brachiopod $\delta^{18}O$ trends and (*k*) brachiopod $\delta^{13}C$ trends (running means for a 3-Ma window and 1-Ma steps) from the Russian platform and from western and central North America (Grossman et al. 2008) (see sidebar, Marine Carbonates as Proxies of Seawater Conditions). (*l*) Areal extent of lycopsid wetland forests by geographic region, adapted from Cleal & Thomas (2005).

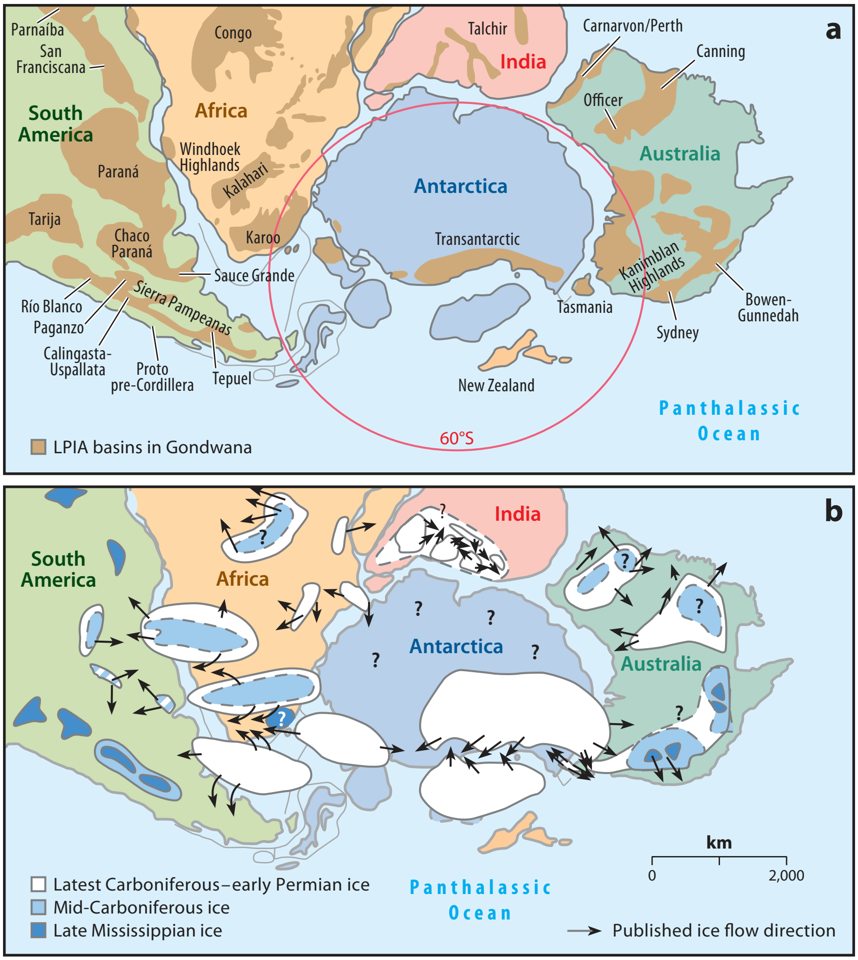

Figure 3

Polar-perspective paleogeographic maps of (*a*) Gondwanan depositional basins and highlands and (*b*) inferred distribution of glacial centers and ice extent during the main stages of glaciation. Figure modified from Isbell et al. (2012). (*b*) Areal extent of latest Carboniferous–early Permian ice (18.6×10^6 km^3) modified for eastern Australia and India using Fielding et al. (2010). Early Permian ice distributed over 21 ice sheets translates to a sea level that is consistent with a maximum glacioeustatic change of 32.5 m (J.L. Isbell, personal communication). Ice extent for the two other glacial stages was inferred from data in Fielding et al. (2008c) and Holz et al. (2010). Glaciation in the Arabian Peninsula (to the north of this reconstruction) would increase the early Permian ice volume (Martin et al. 2008). Dashed boundaries and question marks indicate best (but uncertain) estimates of the geographic positions and extents of ice sheets. Abbreviation: LPIA, late Paleozoic ice age.

life is recorded as a second-order mass extinction (Stanley & Powell 2003) involving catastrophic diversity loss and ecosystem restructuring (Powell 2005, McGhee et al. 2012).

The Carboniferous Glacial Peak

Glacial deposits throughout southern Gondwana record the geographic expansion of continental ice centers during the latest Mississippian through the Middle Pennsylvanian (**Figures 2** and **3**).

Possible sea ice and icebergs in the northern high latitudes are suggested by pebbly mudstones and dropstones from northeastern Siberia (Epshteyn 1981) and China (Shi & Waterhouse 2010). Recent studies of chronostratigraphically constrained high- and low-latitude successions of this age reveal evidence for two, or possibly three, discrete glacial episodes separated by interglacials (**Figure 2**).

Interglacials: 10^5- to 10^6-year periods of contracted ice sheets and rising sea level; possibly ice-free conditions for some intervals

The first peak of ice accumulation occurred at the mid-Carboniferous boundary (323.2 Mya) with ice center development in eastern (Fielding et al. 2008a) and western (Mory et al. 2008) Australia, western central Argentina (Henry et al. 2008, Gulbranson et al. 2010), and possibly the Karoo Basin and the Kalahari Basin of southern Africa (Isbell et al. 2008a) and the Parana Basin of Brazil (Rocha-Campos et al. 2008, Holz et al. 2010). Continental ice was notably absent from Antarctica (**Figures 2** and **3**) (Isbell et al. 2008b). This major phase of glaciation is recorded in midlatitude to low-latitude successions by basin-wide shifts in sedimentation and by the development of erosional valleys, karst surfaces, and, in places, a multimillion-year unconformity (Blake & Beuthin 2008, Rygel et al. 2008, Bishop et al. 2009, Eros et al. 2012b, Martin et al. 2012). Substantial ice accumulation at this time is indicated by a large-scale positive shift in brachiopod $\delta^{18}O$ (Mii et al. 2001) and conodont $\delta^{18}O$ (Buggisch et al. 2008). Notably, this main phase of glaciation coincides with the appearance of lycopsid wetland forests throughout the tropics (**Figure 2**), which was previously attributed to a major cooling event—the Ostrogsky episode described by Durante (2000). A coincident marked increase in seawater $\delta^{13}C$ (**Figure 2**) argues for a major increase in terrestrial C sequestration and a consequent decrease in pCO_2.

The disappearance of glaciers from western-central Argentina by the mid-Bashkirian (Gulbranson et al. 2010, Henry et al. 2010) and the temporary loss of ice in at least eastern Australia (Fielding et al. 2008a) may indicate ice sheet contraction in the later part of the Early Pennsylvanian prior to renewed expansion a few million years later. The long-term sea level provides independent evidence that a decrease in ice volume occurred between these two glacial events, as does a coincident marked decrease in the magnitude (<40 m) of inferred glacioeustatic fluctuations (**Figure 2**).

The second major phase of Pennsylvanian glaciation is recorded by glacial features and deposits throughout the polar to midlatitude basins of Gondwana (**Figure 2**), including both (*a*) renewed glaciation in eastern Australia (Fielding et al. 2008a) and in the Parnaiba Basin and the Parana Basin of Brazil (Caputo et al. 2008, Holz et al. 2010) and (*b*) the onset of glaciation in the Karoo Basin and the Falkland Islands (Visser 1997, Stollhofen et al. 2008) and in the eastern Arabian Peninsula (Martin et al. 2008). Distal glacigenic deposits in Argentina, U-Pb dated to between 315.46 ± 0.07 Mya and 312.82 ± 0.11 Mya, indicate renewed cool or possibly glacial conditions on the western margin of southern Gondwana by the onset of the Middle Pennsylvanian (Gulbranson et al. 2010). Purported Middle Pennsylvanian dropstones in Siberia (Epshteyn 1981) suggest coeval sea ice in the high latitudes of the Northern Hemisphere. In the paleotropical Donets Basin, this second glacial phase is recorded by a prolonged sea-level fall that culminated in an early Moscovian lowstand and the renewed onset of high-magnitude, eccentricity-forced glacioeustasy (Waters & Condon 2012).

Late Carboniferous Global Warming and Deglaciation?

A long-term (~9 Ma) eustatic rise spanned much of the later part of the Middle to Late Pennsylvanian (herein referred to as the late Carboniferous) (**Figure 2**). Several shorter-term (0.8- to 1.6-Ma) lowstands superimposed on this longer-term rise (see, e.g., the late Moscovian and the Desmoinesian-Missourian boundary on the coastal onlap curve in **Figure 2**) have been correlated across hundreds to thousands of kilometers of the Pangean paleotropics (Falcon-Lang et al. 2011, Best et al. 2011, Eros et al. 2012a) and interpreted to record glacial advances paced by long-period modulation of obliquity (Eros et al. 2012b). Although systematic trends in the duration and magnitude of sea-level fall associated with each short-term cycle cannot be correlated to discrete high-latitude glacial events because of chronostratigraphic constraints, Eros et al. (2012b) have interpreted these trends as records of stepwise major contraction of ice sheets during the late Carboniferous. A coincident decrease in $\delta^{18}O$ in brachiopods from the Paleo-Tethys (**Figure 2**) further argues for diminished ice volume (Frank et al. 2008).

The direct record of glaciation (or deglaciation) over this ~9-Ma interval remains equivocal given the paucity of chronostratigraphic constraints (see references in Fielding et al. 2008c). At this time, ice centers may have existed in the Parana Basin, the Kalahari Basin, the Karoo Basin, and possibly India and the eastern Arabian Peninsula (**Figure 2**) (Fielding et al. 2008d). Notably, continental ice was gone from southwestern Gondwana (Limarino et al. 2006, Henry et al. 2010) and eastern Australia (Fielding et al. 2008b). This absence of continental ice, along with the continued absence of glacigenic features and deposits in Antarctica (which was positioned over the South Pole), argues against the presence of large ice sheets in the Southern Hemisphere during the late Carboniferous (Isbell et al. 2012).

Evidence for late Carboniferous warming, associated with onset of aridification across the paleotropics (Tabor & Poulsen 2008, Kabanov et al. 2010), is wide ranging (Dickins 1996, Fielding et al. 2008d, Mory et al. 2008, González & Díaz Saravia 2010). On land, a loss of well-developed coal deposits (Cecil et al. 2003, DiMichele et al. 2009) and a shift in the style of fluvial channel deposits in the southern high latitudes (Gulbranson et al. 2010) and paleotropics (Allen et al. 2011) record a geographically widespread shift to highly seasonal and drier (warm?) climates. The diversity of higher-latitude flora in the Northern Hemisphere (Angara Province) increased significantly, as did that of Gondwanan floras (González 1990, Cleal & Thomas 2005), whereas paleotropical wetland forests declined (**Figure 2**) and underwent an ecological turnover at the Middle to Late Pennsylvanian boundary (DiMichele et al. 2001). In the oceans, a major shift in marine diversity occurred with the introduction of warm-water faunas into parts of southern Gondwana and the cross-hemispheric migration of brachiopods (González & Díaz Saravia 2010, Waterhouse & Shi 2010).

The Early Permian (Cisuralian) Apex of Glaciation

The presence of early Permian glacial deposits in most southern Gondwanan basins (**Figure 2**), including Antarctica (Isbell et al. 2008b), indicates widespread ice sheet accumulation in the Southern Hemisphere. Numerous ice centers (**Figure 3**), from which small to moderate-size ice sheets emanated, developed over highlands throughout the high latitudes and midlatitudes of South America (Rocha-Campos et al. 2008, Holz et al. 2010), southern Africa (Visser 1997, Stollhofen et al. 2008), the Arabian Peninsula (Martin et al. 2008), India (Wopfner & Casshyap 1997), eastern and western Australia (Fielding et al. 2008a, Mory et al. 2008), and the South Asian crustal blocks (Taboada 2010). The extensive glaciomarine deposits of latest Pennsylvanian to early Permian age (Fielding et al. 2008d) indicate that both glaciers and ice sheets in southern Gondwana reached sea level, requiring widespread cooling (Isbell et al. 2012). Inferred dropstones and glaciomarine deposits of early Permian age in the northern paleo–high latitudes suggest that this early Permian climate shift was global (Raymond & Metz 2004). Hypothesized alpine glaciation in the tropics, possibly at low altitudes (500 to 1,000 m), requires a glacial chill well beyond that of the recent past (G.S. Soreghan et al. 2008). Coupled 1–2‰ increases in Paleo-Tethys brachiopod $\delta^{18}O$ and $\delta^{13}C$ across the Permo-Carboniferous boundary interval (**Figure 2**) suggest possible CO_2-driven cooling (Frank et al. 2008). Analogous to the global rise of paleotropical forests during the mid-Carboniferous glacial period, wetland forests on the Chinese and Far Eastern blocks expanded in the earliest Permian (**Figure 2**). A eustatic fall accompanied the earliest Permian apex of glaciation (**Figure 2**), as indicated by both a notable basinward shift of facies and substantial incisions in carbonate-dominated, low-latitude to midlatitude successions (Koch & Frank 2011). Whether substantial ice volume existed in the latest Carboniferous or was restricted to the earliest Permian is debated (Fielding et al. 2008d), and glaciation may have begun earlier in some regions than in others (González & Díaz Saravia 2010, Isbell et al. 2012).

Demise of an Icehouse

The demise of the LPIA is marked by a mid-Sakmarian deglaciation event (**Figure 2**) inferred from marine transgressive deposits and the loss of ice-contact glacial deposits in most Gondwanan basins, including those within the polar circle (Isbell et al. 2003, Fielding et al. 2008c, Lopez-Gamundi & Buatois 2010). However, glacigenic deposits dating from the post-Sakmarian through the end of the middle Permian in eastern (and possibly western) Australia (Fielding et al. 2008a, Mory et al. 2008) and New Zealand (Waterhouse & Shi 2010) indicate continued glaciation in eastern Gondwana until ~260 Mya. The duration and extent of glaciation in Gondwana decreased over time, and ice sheets were replaced by restricted alpine glaciation (Fielding et al. 2008a); this pattern of stepwise deglaciation mirrors the stepped glaciation pattern inferred for the onset of the LPIA (Eros et al. 2012b).

A series of marine transgressions from the mid-Sakmarian through the end of the early Permian recorded in low-latitude successions are evidence of stepwise deglaciation of Gondwana (Montañez et al. 2007, Koch & Frank 2011). Stratigraphic indicators of a diminished magnitude of glacioeustasy (**Figure 2**) and the loss of cyclicity in many successions (see, e.g., Stemmerick 2008) indicate overall dampened glacioeustasy. Deglaciation accompanied the extinction of glacial taxa (Clapham & James 2008, Waterhouse & Shi 2010), the collapse of the Permian paleotropical rainforests (Cleal & Thomas 2005), and the return of steep, pre–ice age latitudinal diversity gradients in the oceans (Powell 2007). Reconstructed atmospheric CO_2 contents indicate greenhouse gas forcing of this icehouse-to-greenhouse turnover (Montañez et al. 2007, Birgenheier et al. 2010).

THE UNRESOLVED ISSUES

The LPIA is one of the best-studied periods of Earth's history. As such, it provides perspective on the global climate system and biosphere responses to major perturbations, including deglaciation. Although its boundary conditions are substantially different from the boundary conditions today, the LPIA may provide a better analog for near-future conditions in a warming-but-glaciated world than the analog provided by the transient warmings of past greenhouse periods. However, much remains to be further understood. Unresolved issues include identifying the climatic forcings that drove glacial-deglacial dynamics, accurately quantifying associated ice volume and eustatic changes, constraining the nature and role of the oceans in the LPIA, and identifying and resolving feedbacks among the atmosphere, ocean, cryosphere, and biosphere. These issues are discussed in the following subsections.

Forcings and Their Influence on Glacial Extent

Any model for the LPIA must account not only for the dynamic glaciation history of the ice age but also for (*a*) the lack of ice at the South Pole during two of the three major phases of ice accumulation in the midlatitudes (**Figure 3**), (*b*) possible ice sheet extensions to ~30°S, (*c*) the intermittent occurrence of sea ice—and possibly glaciers or shelf ice—in the polar Northern Hemisphere, and possibly (*d*) tropical ice proximal to sea level during the latest Pennsylvanian–early Permian apex of glaciation (G.S. Soreghan et al. 2008). Multiple drivers of glaciation have been proposed (for summaries, see Tabor & Poulsen 2008, Isbell et al. 2012), including continental drift over the polar regions, opening and closing of oceanic gateways, tectonically induced variation in the equilibrium line altitude (ELA) for ice, anomalous cold regional conditions produced by coastal upwelling, change in the polar front–subpolar atmospheric circulation, and CO_2-forced cooling.

Continental drift of Gondwana over the South Pole (**Figure 3**), beginning with southwestern Gondwana (Argentina and Patagonia) in the Devonian–Early Mississippian and ending with eastern Gondwana (Australia) in the late Permian, can account for the long-term geographic migration of glacial centers (**Figure 2**) (Eyles 1993, Fielding et al. 2008d, Isbell et al. 2012). Similarly, the early Permian onset of deglaciation has been attributed to a 10–20° northward drift of Pangea (Shi & Waterhouse 2010). This forcing, however, fails to account for several important characteristics of the LPIA. Gradual and generally unidirectional drift would not have led to temporally discrete glacial episodes or intermittent glacial minima; it also fails to explain how the southern polar region remained ice free while glaciers grew at lower latitudes. Conversely, drift cannot explain why eastern Australia underwent stepped deglaciation when it was likely located at the southern pole during the middle to late Permian (Isbell et al. 2012). Paradoxically, the inferred glacial deposits of the northern high latitudes disappeared as Siberia drifted across the polar circle (Blakey 2008).

The closure of the Rheic Ocean between Gondwana and Euramerica (**Figure 1*a***) in the latest Mississippian has been implicated in the initiation of the LPIA (Veevers & Powell 1987, Smith & Read 2000, Saltzman 2003). The closure of the Rheic Gateway is proposed to have cut off the subequatorial current that flowed freely through the tropics, deflecting heat and moisture poleward and providing the precipitation necessary for ice sheet growth on Gondwana. The closing of the Uralian Seaway in the early Permian (Artinskian) would have cut off warm-water currents and moisture to the northern polar region (Shi & Waterhouse 2010), accounting for the loss of diamictites and dropstones in Siberia as it drifted across the northern polar circle. Analogously, closure of the Panama Isthmus has been proposed to explain the onset of Quaternary glaciation in the Northern Hemisphere (see, e.g., Haug & Tiedemann 1998), but numerical climate models provide equivocal support for this idea (Klocker et al. 2005). The deflection of warm currents to polar regions increases precipitation, but it also increases both air temperature and melt potential. Idealized climate model simulations using the FOAM, a coupled ocean-atmosphere model, to test the climate response to a low-latitude Pangean gateway are consistent with increases in surface temperature (by ∼0–2°C) over southern Gondwana, but they indicate very little change in snow accumulation.

Tectonically forced glaciation (or deglaciation) through the creation (or destruction) of topography above the ELA, first proposed by Veevers & Powell (1987) and Eyles (1993), has regained popularity as an important forcing of LPIA glaciations (Isbell et al. 2012). The ELA, the elevation at which ice accumulation and ablation rates are equal, is governed by topography, local heat flux, and climatic conditions. Topography-induced regional changes in the ELA, induced by topography, could resolve the paradox of ice-free poles during times of glaciation throughout the higher midlatitudes. For example, Middle to Late Mississippian glaciation may have been driven by the uplift of the Argentinean Protoprecordillera along the tectonically active Panthalassic margin of Gondwana (Limarino et al. 2006, Henry et al. 2010) and by uplift along the Tasman Fold Belt of eastern Australia (Isbell et al. 2012). In turn, mid-Bashkirian deglaciation in Argentina, which coincides with the development of ice centers in Brazil and southern Africa, can be attributed to extensional collapse driven by plate subduction on the Panthalassic margin. Although this idea is compelling because it accounts for regional ice centers without requiring massive ice sheets, climate model simulations indicate that topography may not have been a necessary condition for the development and demise of Gondwanan ice sheets (Otto-Bliesner 1996, Horton & Poulsen

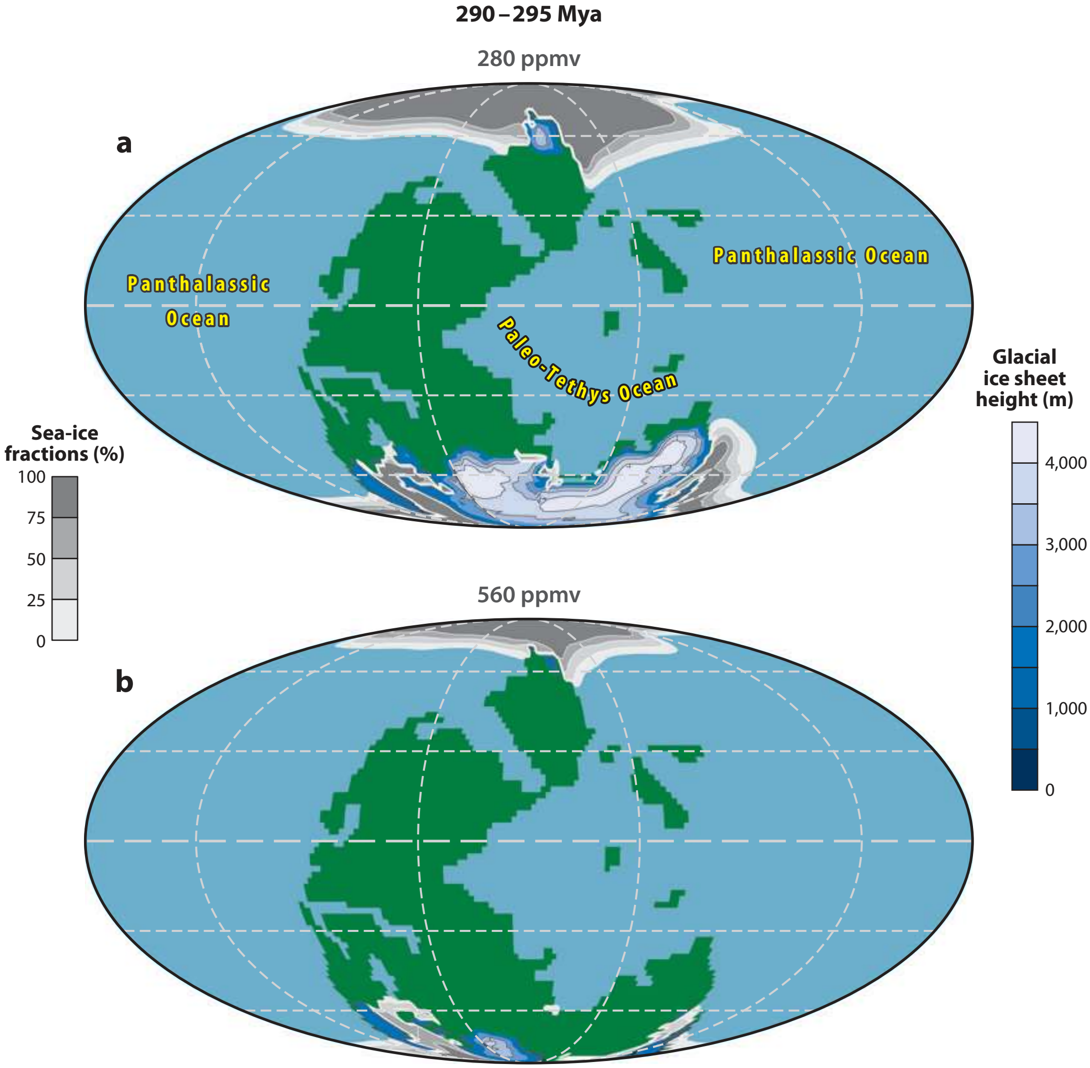

Figure 4

Simulated maximum glacial ice heights (in m; indicated by blue shading) and sea-ice fractions (in %; indicated by gray shading) at CO_2 levels of (*a*) 280 ppmv and (*b*) 560 ppmv. The 5-ka (1 ka = 1,000 years) snapshots shown here represent maximum Gondwanan ice volumes simulated over an ~240-ka period with varying orbital parameters. Note the simulation of both small continental ice sheets and coastal sea ice in the Northern Hemisphere of Pangea; these features persist throughout the ~240-ka simulations. For full details of these simulations, see Horton et al. (2010, 2012).

2009, Horton et al. 2010). Climate–ice sheet models of the LPIA with overall low topography (<1,100 m) simulate multiple ice centers that correspond well with the timing and distribution of glacigenic deposits (**Figure 4*b***). Notably, in simulations that evaluate decreasing atmospheric CO_2 levels, ice centers in South America and Australia first nucleate at higher CO_2 levels [560 parts per million by volume (ppmv)] (Horton & Poulsen 2009), likely because these ice centers are proximal to the coast, which is a ready moisture source, and subsequently expand to the polar circle regions of southern Africa and Antarctica when global CO_2 levels drop to ≪560 ppmv (**Figure 4**).

Eyles (1993) first suggested a dramatic drop in atmospheric CO_2 through the early Carboniferous, which may have occurred due to C sequestration by expanding wetland forests and accelerated rates of continental (silicate) weathering, as the likely driver for the LPIA. The earliest short-lived glaciations in the Mississippian, however, predated both the expansion of lycopsid paleotropical forests (Cleal & Thomas 2005) and a positive $\delta^{13}C$ shift interpreted to record a large increase in organic C sequestration (**Figure 2**) (Frank et al. 2008) by >10 Ma. This lagged response may indicate that CO_2 drawdown did not trigger glaciation, or it may record vegetation-climate feedbacks. Sea-level drawdown by initial ice sheets under falling atmospheric CO_2 levels may have promoted the expansion of lowland forests, which in turn amplified CO_2 drawdown and the expansion of continental ice (Cleal & Thomas 2005). Analogous to the onset of Cenozoic glaciation, the stepped buildup of the Carboniferous ice sheets inferred from the sea-level history for this time (Eros et al. 2012b) is consistent with the CO_2 threshold behavior exhibited by climate–ice sheet models of the LPIA (Horton et al. 2010).

Global warming and ice sheet contraction during the late Carboniferous also may have been linked to CO_2. The contraction of the wetland forests during this time would have resulted in a 50-fold reduction in CO_2 sequestration (Cleal et al. 1999). Fluctuating CO_2 levels through the early to middle Permian have been further invoked to explain the earliest Permian apex of glaciation and the ensuing stepwise deglaciation of the LPIA (Montañez et al. 2007).

Climate–ice sheet models support the idea that atmospheric CO_2 was the fundamental driver for the buildup and demise of the ice sheets (Crowley & Baum 1992). According to these models, the initiation and expansion of Gondwanan ice sheets are highly sensitive to the atmospheric CO_2 level (Hyde et al. 1999; Horton et al. 2007, 2010; Horton & Poulsen 2009); substantial ice volume develops at CO_2 levels of 560 ppmv or less (**Figure 4**). The CO_2 threshold for deglaciation is more difficult to constrain because it depends strongly on the extent, height, and location of the ice sheets. Deglaciation of a single, massive ice sheet on southern Gondwana may require CO_2 levels in excess of 2,240 ppmv (Horton & Poulsen 2009). In contrast, the melting of smaller distributed ice sheets would require much smaller increases in atmospheric CO_2.

Climate and climate–ice sheet models may provide further constraints on the paleoatmospheric CO_2 levels of the LPIA. Climate–ice sheet models predict glaciation at CO_2 values that are less than 560 ppmv (**Figure 4*b***), whereas at 280 ppmv, distributed ice centers coalesce to form a single massive ice sheet that extends across Antarctica, southern Africa, southern Australia, and India (**Figure 4*a***). This result appears to be consistent across a range of models (e.g., Otto-Bliesner 1996, Hyde et al. 1999, Horton & Poulsen 2009). To confirm these model-defined thresholds, future refinements of both the timing of glaciation and the timing and magnitudes of CO_2 transitions are critical.

Despite their potential for perturbing heat and moisture fluxes in the regions of ice accumulation, neither regional shifts in atmospheric circulation nor the development of superupwelling zones along specific margins has been fully considered. Although these forcings are not likely to initiate widespread hemispheric glaciation, they may have affected glaciation on a regional scale. The persistence of eastern Australian glaciation through the middle Permian, after the deglaciation of the rest of Gondwanaland, could record coastal upwelling of cold waters, an interpretation consistent with the likely direction of the prevailing winds (cf. Jones et al. 2006). The distribution and size of ice centers may also have been influenced by changes in regional atmospheric circulation over southern Gondwana as a consequence of either ice sheet development or other forcings. Investigations of the Quaternary Laurentide Ice Sheet suggest that the intensification of anticyclonic flow over the growing ice sheet substantially influenced heat fluxes along its margins, thereby influencing its shape and size (Roe & Lindzen 2001, Herrington & Poulsen 2012). Similar atmosphere–ice sheet feedbacks over Gondwana would have promoted glacial expansion along western ice margins and the stabilization of eastern margins in addition to generally promoting the development of ice centers rather than a single, massive ice sheet. Notably, climate simulations of Gondwanan ice that do not incorporate atmospheric circulation tend to simulate a single, massive ice sheet (Hyde et al. 1999), whereas those that do incorporate atmospheric circulation simulate multiple ice centers (Horton et al. 2007).

Climate and climate–ice sheet models generally support the possibility of continental ice sheets and sea ice in the northern polar region at CO_2 levels of less than 1,120 ppmv (**Figure 4**) (Otto-Bliesner 1996, Hyde et al. 2006; D.E. Horton, C.J. Poulsen, D. Pollard, unpublished data) with the susceptibility to glaciation increasing as Siberia migrated northward during the late Paleozoic. In fact, these models suggest that the absence of northern polar ice may require high atmospheric CO_2 levels that are inconsistent with proxy CO_2 reconstructions. In contrast, climate models underscore the challenge of growing low-latitude (<3,000 m) glaciers near sea level. Even under minimum CO_2 levels (140 ppmv), late Paleozoic maximum monthly surface temperatures in the tropics reach 20–25°C, which are well above freezing (G.S. Soreghan et al. 2008). Perhaps the most compelling argument against low-elevation, low-latitude glaciation is that potentially severe conditions, including widespread glaciation in the Northern Hemisphere, would be implied for the rest of Pangea, but no evidence for such conditions currently exists.

Ice Volume and Stability and the Eustatic Response

A range of methods applied to near-field glacial and far-field stratigraphic records, as well as numerical modeling, have been used to reconstruct ice volume and glacioeustasy through the LPIA. Early estimates of $\sim 39.8 \times 10^6$ km^3, equivalent to an isostatically adjusted glacioeustatic component of 60 ± 15 m (Crowley & Baum 1991), were derived using Quaternary ice area–volume relationships and geologic evidence of peak Gondwanan ice area. Noting the discrepancy between the estimates from this method and those from far-field evidence, Crowley & Baum (1991) argued that a lower value is more consistent with evidence that Gondwanan ice was never united into one massive sheet. More recent estimates of ice volume (**Figure 3**) based on the areal distribution and hypothesized number of ice sheets inferred from high-latitude glacial deposits indicate a maximum estimate of $20\,(\pm 2) \times 10^6$ km^3 during the apex of glaciation, nearly half that proposed by Crowley & Baum (1991). These estimates, however, remain poorly constrained given the uncertainties in chronostratigraphy and about the extent and type of ice [e.g., ice sheet(s), caps, or glaciers] for some regions of Gondwana and the potential for erosion of older deposits by advancing ice (but see Isbell et al. 2003, 2008a).

It has been argued that the magnitudes of eustatic change inferred from low-latitude successions are a more sensitive proxy for ice volume than the geographic distribution of high-latitude glacial deposits because they record changes in global mean sea level, which integrates all global changes in ice volume for a given interval of time. A recent compilation (Rygel et al. 2008) of estimates of high-frequency sea-level fluctuations inferred from cyclothems, stratigraphic relationships and incised valleys, and, to a lesser extent, geochemical proxies from low-latitude Permo-Carboniferous successions illustrates the substantial variability in the magnitudes of eustatic change through the LPIA (**Figure 2**). The variability through time of the estimated magnitudes ranges between 10 and ≥200 m, with more recent cycle and sequence stratigraphic studies suggesting a slightly smaller range of <20 m to 70 m (Bishop et al. 2010, Best et al. 2011, Martin et al. 2012, Waters & Condon 2012). Inferred magnitudes greater than ∼50 m, however, may be problematic given the growing support for numerous ice centers (up to 20 during the glacial peak) from which small ice sheets and glaciers emanated (**Figure 5**).

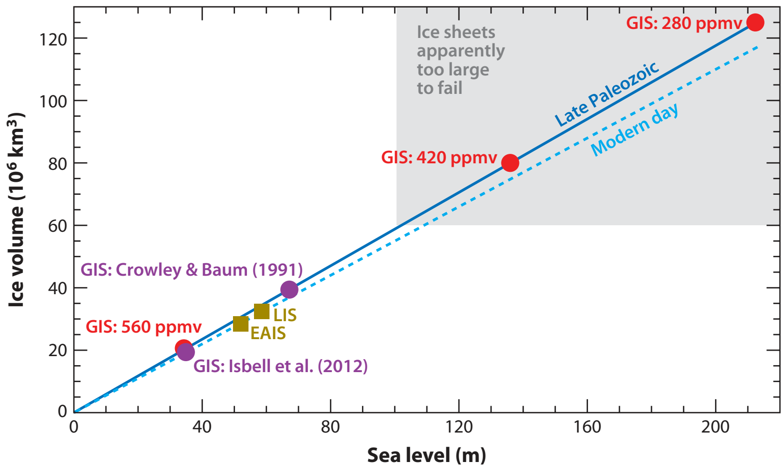

Figure 5

Glacial ice volume versus isostatically adjusted sea level for the late Paleozoic ice age (*solid dark blue line*) and modern day (*dashed light blue line*). A comparatively larger ocean volume in the Permo-Carboniferous than in the modern era leads to slightly smaller glacioeustatic responses to changes in ice volume. Solid purple and red circles indicate Gondwanan ice sheet (GIS) volumes based on, respectively, the distribution of glacigenic deposits (Crowley & Baum 1991; J.L. Isbell, personal communication) and estimates from climate model simulations [560, 420, 280 ppmv from Horton & Poulsen (2009); 280 ppmv from Hyde et al. (1999)]. For comparison, brown squares show Quaternary Wisconsin glaciation ice volumes for the East Antarctic Ice Sheet (EAIS) and the Laurentide Ice Sheet (LIS) from Hughes et al. (1981). At CO_2 values <560 ppmv, simulated Gondwanan ice sheets coalesce into a single sheet that is too large to ablate through orbital forcing (Horton & Poulsen 2009). Gray shading represents the region for which the ice sheets are apparently too large to fail.

Perhaps most importantly, magnitudes of eustatic change vary not only through time but also by tens of meters to well over a hundred meters within some narrow intervals (**Figure 2**). Some of the inter- and intra-interval variability in eustatic magnitudes likely reflects the uncertainty involved in using some stratigraphic records to make these estimates. Several factors may lead to overestimates, such as the possibility of anomalously shallow pycnoclines (less than or equal to a few tens of meters) in late Paleozoic epeiric seas [e.g., the Midcontinent Sea in the United States (Bishop et al. 2010)] and the complex nature of stacked incised valleys in stratigraphic successions (Fischbein et al. 2009). The superposition in cyclothems of erosion surfaces and paleosols over black, laminated shales, interpreted to have formed below the oceanic pycnocline, has led to inferred sea-level changes of 100 to 200 m (see, e.g., Heckel 1977, 1994). In part, these eustatic inferences are based on a modern blue-water model in which the pycnocline is at least 200 m deep. Epicontinental seas, however, may not fit this model. Because these seas had relatively shallow bathymetry, long residence times of water masses (Peters 2007), and the potential to develop shallow pycnoclines during wet periods (Algeo & Heckel 2008), water depths as shallow as a few tens of meters were required to produce the observed juxtaposition of facies.

Blue water: marine water environments that lie seaward of the coastal shallow ocean and extend to the global deep ocean underlain by oceanic crust

Some of the largest magnitudes (100 to ≥150 m) of eustatic change have been inferred from intracyclothemic shifts in conodont $\delta^{18}O$ (**Figure 2**) (Joachimski et al. 2006, Elrick & Scott 2010). These magnitudes may be overestimated given that conodont $\delta^{18}O$ is influenced by both ambient seawater temperature and $\delta^{18}O$ composition. The effects of variation in the evaporation-to-precipitation ratio and in freshwater influx on epeiric seawater salinity (and $\delta^{18}O$) have not been accounted for in these estimates despite their potential to impart a strong signature on conodont $\delta^{18}O$ (Bates et al. 2011, cf. Peters 2007).

In general, intervals of the largest inferred magnitudes (>50 m) coincide with the main glacial phases and periods of major lowstands, and vice versa (**Figure 2**). Existing estimates of ice volume based on inferred magnitudes of eustatic change should be considered maximum values given that few estimates account for processes that would respond to the same climate forcing(s) that drive changes in ice volume, such as the thermal expansion of seawater and the filling and draining of continental lakes and reservoirs, and that would ultimately lead to sea-level changes of a few meters to tens of meters (Jacobs & Sahagian 1993).

Attempts to simulate orbitally forced changes in LPIA ice volume and glacioeustasy using climate–ice sheet models have been instructive, if not entirely successful. Using a two-dimensional energy balance model and a two-dimensional, vertically integrated ice sheet model (without incorporating atmospheric circulation), Hyde et al. (1999) simulated a single, massive ($\sim 125 \times 10^6$ km^3) Gondwanan ice sheet centered on the South Pole that experienced very large orbitally forced changes in ice volume through ablation on its periphery. The simulated changes in ice volume were equivalent to ~100–125-m changes in sea level. Although this simulation compared well with geological observations at the time of the aforementioned study, as summarized above, more recent field studies argue that a single, massive ice sheet is untenable. At atmospheric CO_2 levels of 560 ppmv, the same study simulated a Gondwanan ice sheet up to three times larger than more recent ice volume estimates that yielded substantially lower magnitudes of sea-level change (<50 m).

More recent modeling efforts (Horton et al. 2010) using an atmospheric general circulation model coupled to a three-dimensional ice sheet model simulate smaller ice volumes ($\sim 20 \times 10^6$ km^3 with CO_2 values of 560 ppmv) distributed as multiple ice centers (**Figure 4*b***). Although these simulations compare well with maximum ice volume estimates based on glacigenic deposits of the LPIA (**Figure 3*b***), they generate orbitally forced ice volume changes equivalent to ~25 m of sea-level change. Thus, these simulations suggest a contradiction between glacigenic evidence for distributed (multiple) ice sheets (**Figure 3**) and stratigraphic evidence for large (≥100 m) short-term glacioeustatic changes (**Figure 2**). Moreover, recent climate–ice sheet modeling studies (Horton & Poulsen 2009, Horton et al. 2010) indicate that orbital forcing alone is not sufficient to cause the waxing and waning of a massive Gondwanan ice sheet. Simulated ice sheets with large volumes ($>60 \times 10^6$ km^3) do not ablate during warm summer orbits due to their high, and therefore very cold, surfaces. Thus, they present a paradox—these ice sheets sequester sufficient water to account for the large glacioeustatic changes inferred from cyclothems, but they are too large and too stable to respond to orbital forcing (**Figure 5**). This too-large-to-fail paradox may seem to belie the existence of Pleistocene glacial-interglacial cycles, but the Laurentide Ice Sheet was significantly smaller (30.9–34.8×10^6 km^3) (Hughes et al. 1981) than the massive Gondwanan ice sheet simulated in these studies. As mentioned above, orbitally forced glacioeustatic changes of ~25 m were simulated when smaller ice volumes similar to that of the Laurentide Ice Sheet occupied Gondwana (Horton et al. 2010). These results support the notion that periods of major glaciation inferred from longer-term sea-level lowstands associated with high-magnitude glacioeustatic fluctuations (e.g., the mid-Carboniferous and Early-Middle Pennsylvanian boundary intervals in **Figure 2**) were likely characterized by the existence of numerous distributed smaller ice sheets.

Notably, in Horton et al. (2010), orbitally forced insolation changes alone were not sufficient to drive ice sheet growth and decay. Vegetation-insolation feedbacks at the ice margin, including the expansion of tundra during insolation minima and of barren ground during insolation maxima, were pivotal in causing local cooling and warming that ultimately led to ice expansion and retraction. These modeling results underscore the need to more fully investigate feedbacks associated with Earth's orbital fluctuations, including, for example, changes in greenhouse gas levels, physiological forcing by vegetation, dust loading, and ocean circulation. The physical processes governing the collapse of continental ice sheets also require further exploration. Although the model used in Horton et al. (2010, 2012) incorporates important processes, including ablation, subglacial melting and sliding, and calving, other processes have yet to be investigated, including subglacial till formation and deformation and interactions between continental ice sheets and marine ice shelves.

The State of the Oceans

Major changes in ocean circulation occurred with the closing and opening of gateways and the expansion and contraction of Gondwanan ice sheets (Saltzman 2003, Reid et al. 2007, Shi & Waterhouse 2010). Faunal migration patterns inferred from paleogeographic distributions of climate-sensitive marine fauna, primarily brachiopods, have been used to reconstruct surface current configurations in the Paleo-Tethys and Panthalassic Oceans (**Figure 1*a***) (see, e.g., Reid et al. 2007, Clapham 2010). The hypothesized contraction of the southward-flowing, warm currents of the southern Paleo-Tethys gyre that coincided with the expansion of the southern polar front during peak glacial phases is considered analogous to that of recent glacial oceans (Angiolini et al. 2007). The proposed introduction of northward-directed, deep cold-water currents into the low-latitude Panthalassic Ocean, perhaps in step with the expansion of Gondwanan ice sheets (Waterhouse & Shi 2010), however, has no Pleistocene glacial analog (H. Spero, personal communication).

Significantly, the tropics are hypothesized to have remained climatically buffered (25°C ± 5°C), even during the postulated early Permian apex of glaciation (Shi & Chen 2006). In contrast to paleobiologic inferences of greatly reduced warm-tropical faunal niches (Powell 2005, 2007), this notion of equable tropical oceans during the LPIA is supported by surface-water temperatures inferred from shallow-water fossil $\delta^{18}O$ compositions (see, e.g., Mii et al. 2001, Buggisch et al. 2008, Angiolini et al. 2009). Conversely, Permo-Carboniferous brachiopod Mg/Ca and $\delta^{18}O$ have been used to argue for shallow-water temperatures of glacial tropical oceans that were significantly colder (up to 10°C) than their modern counterparts (Powell et al. 2009, Giles 2012). This would suggest much larger swings in shallow-ocean temperatures during the LPIA than during glacial-interglacial cycles of the Late Pleistocene (~3°C ± 0.5°C) (Ballantyne et al. 2005).

In many ways, the thermal state of the LPIA tropics is fundamental to understanding the severity of high-latitude climate and the degree to which the lack of warm-tropical niches led to the sustained low biodiversity and evolutionary turnover rates in marine ecosystems (Stanley & Powell 2003, Powell 2005). Climate models do not generally indicate climatically buffered tropics in the Permo-Carboniferous (Winguth et al. 2002, Kiehl & Shields 2005, Peyser & Poulsen 2008); rather, these models document high-latitude climate change that propagates through momentum, heat, and moisture fluxes to the tropics via the atmosphere and the ocean. The magnitude of tropical climate change in these models is very much a slave to the high-latitude forcing. Large climate forcings, such as the growth of an expansive Gondwanan ice sheet to nearly 30–40°S, would have been strongly felt in the tropics as a drop in surface temperature of up to 4°C (Peyser & Poulsen 2008). Conversely, the orbitally driven climate-ice simulations of Horton et al. (2010), which generate numerous smaller ice sheets, predict low-latitude surface temperature changes of <2°C on land and <0.5°C in the ocean (**Figure 6*a***). The apparent absence of significant glacial-interglacial tropical temperature changes seen in these models, in accordance with marine fossil $\delta^{18}O$ levels, may provide indirect evidence that Gondwanan ice volumes were smaller than traditionally believed. The aforementioned large tropical surface temperature changes inferred

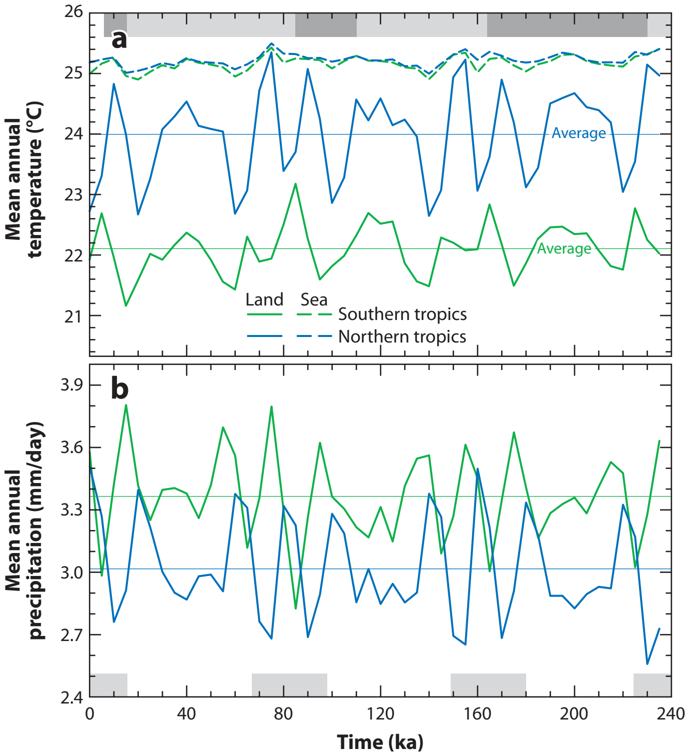

Figure 6

Simulated late Paleozoic ice age mean annual temperature and mean annual precipitation based on a climate–ice sheet model with varying orbital parameters and a CO_2 level of 560 ppmv (Horton et al. 2010, 2012). (*a*) Mean annual land (*solid lines*) and ocean (*dashed lines*) surface temperatures (°C) for tropical southern (0–15°S; *green lines*) and northern (0–15°N; *blue lines*) regions. (*b*) Mean annual precipitation (mm/day) over land for tropical southern (0–15°S; *green lines*) and northern (0–15°N; *blue lines*) regions. The simulation was run with idealized orbital cycles of 40 ka (1,000 years = 1 ka) for obliquity, 20 ka for precession, and 80 ka for eccentricity. Periods of high eccentricity (maximum of 0.057) are shaded in gray along the lower *x*-axis. Simulated high-latitude ice volumes are indicated by shading (light shading indicates ice volumes of $<10^7$ km^3; dark shading indicates ice volumes of 1–2 $\times$ 10^7 km^3) along the upper *x*-axis. Surface temperatures and precipitation mainly correspond to low-latitude insolation forcing driven by changes in eccentricity, obliquity, and precession. Northern and southern land temperatures are in phase and higher during periods of lower obliquity and are out of phase when both eccentricity and precession are high. Northern Hemisphere and Southern Hemisphere precipitation levels are generally out of phase, indicating that precipitation is most sensitive to precessional forcing and most variable when eccentricity is high. There is little correspondence between Gondwanan ice volume and low-latitude temperature or precipitation.

from reconstructed brachiopod habitat temperatures would require more severe high-latitude forcing, possibly including large swings in both ice volume and atmospheric CO_2.

The hypothesized free interchange of cool-water brachiopods between the high latitudes of both hemispheres during glacial periods of the LPIA (Waterhouse & Shi 2010) and the purported occurrence of cold-water (≤7°C) precipitates in paleotropical successions (Brandley & Krause 1997) suggest the possibility of anomalously cold low-latitude surface oceans. Ocean simulations of the late (Kiehl & Shields 2005) and middle Permian (Winguth et al. 2002) predict upwelling and cooler surface temperatures along the eastern Panthalassic Ocean and on the lee side of the South China block until the Paleo-Tethys becomes confined in the late

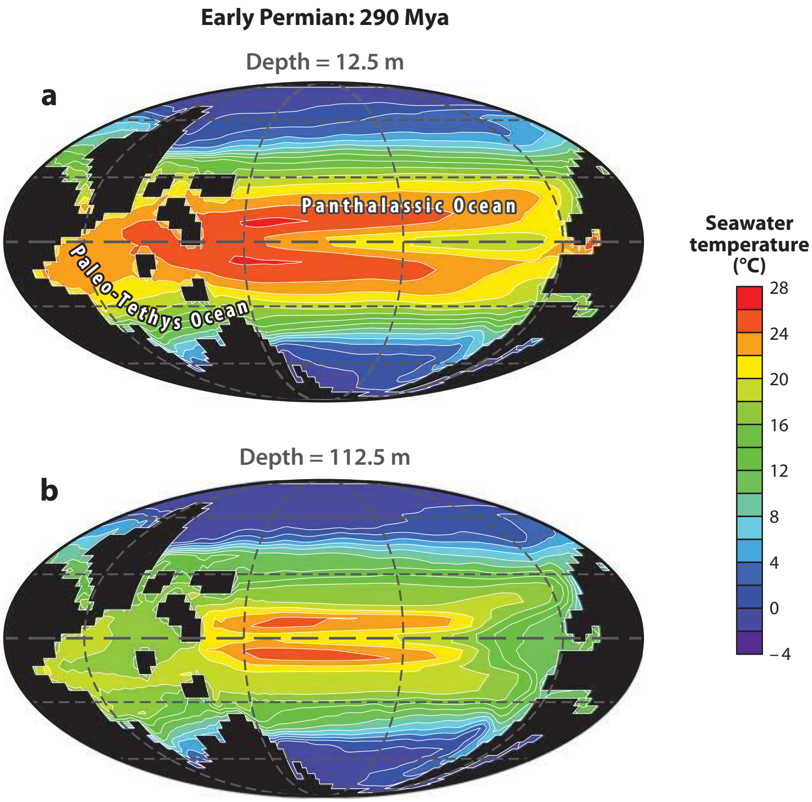

Figure 7

Simulated early Permian mean annual seawater temperatures (°C) (*a*) near the surface and (*b*) at a depth of approximately 100 m. The low-latitude Panthalassic Ocean has a prominent warm pool (with temperatures >24°C) in the west and an upwelling zone in the east. In the subsurface (*b*), cold water penetration toward the equator can be seen along the eastern basins in both the Panthalassic and Paleo-Tethys Oceans. Encroachment of these cold temperatures creates a strong thermocline at shallow depths in these regions. Black shading represents continents. This early Permian simulation was performed using the GENMOM coupled ocean-atmosphere model and a similar methodology to that outlined in Zhou et al. (2008). CO_2 values of 280 ppmv were prescribed; other trace gases were set to preindustrial values. The solar constant was ~97.5% of its modern value.

Permian (Kiehl & Shields 2005). Our own coupled ocean-atmosphere simulations of the early Permian also indicate strong upwelling on the eastern margins of both ocean basins (**Figure 7**). Notably, cold waters sourced from along the sea-ice line of the Northern Hemisphere enter the eastern Pacific upwelling zone and even penetrate the North American epicontinental seaway, setting up a sharp, shallow thermocline in these tropical regions. The intensification of the low-latitude thermocline is likely a general feature of high-latitude cooling and equatorward advection of polar waters (see, e.g., Lee & Poulsen 2006) and may explain the presence of low-latitude cold-water indicators at the subsurface. In this case, the cold temperatures inferred from late Paleozoic brachiopods (Powell et al. 2009), which lived at depths of up to hundreds of meters, could be compatible with the warmer shallow-water temperatures inferred from coeval fossil $\delta^{18}O$ compositions without the invocation of large swings in ice volume or atmospheric CO_2.

Latitudinal temperature gradients (LTGs) are poorly constrained due to the dearth of seawater temperature proxy data for the late Paleozoic high latitudes. During the final stage of the late Paleozoic ice age, LTG estimates based on brachiopod $\delta^{18}O$ values (Korte et al. 2008, Mii et al. 2012) and marine faunal distribution (Angiolini et al. 2007) indicate an LTG similar to that of the modern surface oceans (14°C). Whether LTGs decreased with turnover to a greenhouse world, as documented for other periods of warming (Montañez et al. 2011), remains uncertain, as do the roles of ocean circulation and heat transport in setting the late Paleozoic LTGs. Smith & Read (2000) and Saltzman (2003) have hypothesized that the mid-Carboniferous closure of the Rheic Seaway intensified the western boundary current along eastern Gondwana, enhancing heat and vapor transports to southern Gondwana, but, to our knowledge, this idea has not been tested using climate models. Modeling studies of the middle and late Permian (with possible implications for the LPIA because of their geographic similarities) report subtropical gyres and meridional ocean heat transports that are greater than those of the modern era (Kutzbach & Guetter 1990, Winguth et al. 2002, Kiehl & Shields 2005) and that contribute to high-latitude warming. All else being equal, these studies indicate that the late Paleozoic would have had a more equable climate due to larger ocean heat transports; however, the influence of Gondwanan glaciation and changing atmospheric CO_2 levels on ocean circulation and heat transports has yet to be appropriately explored.

Atmospheric Response and Linkages Between Low and High Latitudes

Teleconnections between high-latitude ice sheet behavior and low-latitude atmospheric dynamics during the late Paleozoic have been proposed largely on the basis of reconstructed shifts in the tropical continental climate that are consistent with orbital-scale glacial-interglacial cycles (summarized by Rankey 1997, Falcon-Lang & DiMichele 2010, Horton et al. 2012). The discovery of discrete, million-year glacial events and intermittent glacial minima has allowed evidence of contemporaneous low-latitude climate shifts at a comparable timescale to emerge (see, e.g., Feldman et al. 2005, Roscher & Schneider 2006, Birgenheier et al. 2009, Allen et al. 2011, Eros et al. 2012b). Disparity in the inferred polarity of climate changes during glacials and intermittent interglacials at all timescales has led to a range of conceptual models of glaciation-glacioeustasy-climate linkages. Some models suggest that glacials were relatively drier and less seasonal than interglacials (see, e.g., Soreghan 1994, Tandon & Gibling 1994, Olszewski & Patzkowsky 2008), whereas others argue for humid glacial climates with greatly dampened seasonality and drier, highly seasonal interglacials (Perlmutter & Matthews 1989, Miller et al. 1996, Cecil et al. 2003). Still other studies suggest that significant climate change in the low latitudes may have been linked to times of glacial-interglacial turnover (i.e., transgressions, late glacials with maximum ice accumulation) (Falcon-Lang & DiMichele 2010, Eros et al. 2012b). Our numeric modeling results indicate that many conceptual models of ice sheet–low-latitude climate linkages likely oversimplify the processes that governed climate variability in the Pangean paleotropics (Poulsen et al. 2007, Peyser & Poulsen 2008, Horton et al. 2012).

The nature of low-latitude climate change may have varied with the timescale (10^4 to 10^6 years) of cyclicity, through time, and in response to specific forcings. Through a series of sensitivity experiments with specified Gondwanan ice sheets, Peyser & Poulsen (2008) showed that both the Hadley circulation and low-latitude convective precipitation responded to cross-hemispheric LTGs; more intense summer precipitation and more intense total precipitation in the Northern Hemisphere occurred during times of expansive glaciation and large temperature gradients, regardless of timescale. In comparison, Horton et al. (2012) reported that in the absence of large Gondwanan ice sheets and substantial ice sheet expansion and contraction, low-latitude precipitation responded primarily to orbital forcing, not ice volume (**Figure 6*b***). These and other studies underscore the need to better resolve the conditions of the LPIA, specifically the geographic extent and timing of Gondwanan glaciation, in order to fully understand linkages between low and high latitudes during glacial-interglacial intervals. Climate simulations further illustrate how ice volume, glacioeustasy, and low-latitude precipitation may fluctuate on similar orbital timescales without being directly linked (Horton et al. 2012), a finding that is contrary to what has been widely argued. Notably, climate models support the conclusion that on timescales that are longer than orbital scale, low-latitude precipitation was likely controlled by atmospheric CO_2 levels. Climate models indicate that as CO_2 levels rose through the Permian demise of the LPIA (see, e.g., Montañez et al. 2007), higher tropical surface temperatures would have enhanced evaporation rates over land, causing reductions in both soil moisture and wet season length and an expansion of the desert biome (Poulsen et al. 2007, Horton et al. 2012) as observed in paleosols throughout the early Permian paleotropics (Tabor et al. 2008).

Linkages have also been drawn between monsoonal circulation on Pangea and the waxing and waning of Gondwanan ice sheets. Due to its immense landmass, the Pangean supercontinent was prone to large seasonal changes in heating that would have driven intense monsoons, namely the megamonsoons described by Kutzbach & Gallimore (1989). Although monsoons were likely present in the subtropics of both hemispheres, they were strongest in the Southern Hemisphere because of the asymmetry in land distribution between the hemispheres (Kutzbach & Gallimore 1989, Peyser & Poulsen 2008, Horton et al. 2012). The intensity of monsoonal circulation in the Pangean equatorial region has been linked to eccentricity-scale glacial-interglacial changes in atmospheric circulation, although the polarity of climate change differs between empirical studies (Miller et al. 1996, M.J. Soreghan et al. 2008). In climate simulations (see figure 7 in Peyser & Poulsen 2008), glaciation of southern Gondwana substantially alters the balance of the seasonal subtropical monsoons in the Southern Hemisphere, strengthening the winter high-pressure system and weakening the low-pressure system. In turn, these changes affect seasonal cross-equatorial moisture transport, enhancing northward flow during the boreal summer and reducing southward flow in the boreal winter. The net result of these changes is to enhance annual precipitation in the northern low latitudes during glacials and to reduce it during interglacials.

SUMMARY POINTS

1. The view of the late Paleozoic has evolved from one of long-term stability to one of dynamic change that archives the climate and ecosystem response to repeated glacial-interglacial conditions that were likely CO_2 forced. As the most recent transition from an icehouse to a greenhouse world, the late Paleozoic provides a unique analog for our warming world.
2. Both the stepped nature of glaciation during the onset and demise of the LPIA and the temporal distribution of ice centers suggest threshold behavior, likely involving changes in atmospheric pCO_2 and orbital forcing analogous to that which occurred during the initiation of the Cenozoic icehouse. Climate model simulations indicate that CO_2 was the fundamental driver for the buildup and breakdown of glaciers. Other factors, including topography, may have been locally important.

3. Field and model evidence argue for total ice volumes ($\sim 20 \times 10^6$ km^3) that are smaller than previously suggested and distributed among multiple ice centers. This evidence also supports the possibility of bipolar glaciation at times, although both the nature and extent of Northern Hemisphere ice remains elusive. Low-latitude glaciers near sea level (<3,000 m) remain problematic given the warm low elevations simulated by models and the geological evidence for a stable tropical climate.
4. Glacioeustatic responses to the waxing and waning of continental ice were likely less extreme than previously suggested ($\leq$50 m versus up to $\geq$150 m) given both the smaller total ice volume of multiple smaller ice sheets and glaciers and the insensitivity of massive ice sheets to orbital forcing. The large temporal variability in the inferred magnitudes of glacioeustasy in part records differences in ice volume and stability during glacial events and intermittent periods of ice contraction, and it highlights the problem of extrapolating glacioeustasy magnitudes from a specific stratigraphic interval to longer periods of the LPIA.
5. Geographic patterns of diversity and the community composition of marine fauna argue for major changes in ocean circulation as the Pangean supercontinent developed and the extent of continental glaciation changed. Geochemical and modeling evidence about the LPIA oceans is needed to shed light on the roles of ocean circulation and ocean heat transport in mediating LPIA climate change and influencing marine diversification and evolutionary turnover rates.
6. Stratigraphic and climate modeling studies reveal the potential for strong teleconnections between high-latitude ice sheet behavior and low-latitude atmospheric dynamics at orbital (10 ka to ~1–2 Ma; 1 ka = 1,000 years) timescales. The response of the low-latitude climate, however, would have varied with specific forcing(s) and the degree to which a given forcing dominated—all a function of timescale and magnitude of perturbation. On longer timescales, atmospheric $p\mathrm{CO_2}$ was the dominant influence on the low-latitude climate.

FUTURE ISSUES

1. Improved chronostratigraphy of glacial deposits, particularly for regions that may have hosted large ice volumes (e.g., eastern South America, southern Africa, western Australia), is needed to establish the degree of synchroneity of glaciation at a sub-Ma resolution and to improve estimates of ice volume throughout the LPIA.
2. Data–climate model studies (especially those with a focus on the forcings of and climate thresholds for the growth and demise of continental ice), the feedbacks associated with Earth's orbital fluctuations and terrestrial vegetation, and the influence of Gondwanan glaciation and gateways on ocean circulation and heat transport should be expanded and applied to the resolution of the LPIA issues presented in this review. These issues include the ice volume–glacioeustasy paradox; the persistence of midlatitude ice while the southern polar region remained ice free; the role of ocean circulation and ocean heat transport in mediating climate and biotic change; and the nature of mechanistic linkages between climate, ice extent, and glacioeustasy.

3. Future proxy studies that focus on improved estimates of the parameters required for data–climate model comparisons are much needed, including shallow-ocean temperatures across the paleolatitudes; higher precision, accuracy, and resolution of paleoatmospheric CO_2 records that are chronostratigraphically tied to glacial and eustatic events; controls on seawater $\delta^{18}O$ in epeiric seas, particularly in conjunction with climate change; and refined estimates of the composition, distribution, and ecosystem physiology of terrestrial floral communities.

DISCLOSURE STATEMENT

The authors are not aware of any affiliations, memberships, funding, or financial holdings that might be perceived as affecting the objectivity of this review.

ACKNOWLEDGMENTS

Financial support was provided by the US National Science Foundation (EAR0545654, OISE0826105, and EAR1024737 to I.P.M. and EAR0544760 to C.J.P.). The manuscript was prepared while I.P.M. was a Guggenheim Fellow. The authors thank the following colleagues for sharing their expertise and insight: Vladimir Davydov, Bill DiMichele, J. Michael Eros, Erik Gulbranson, Dan Horton, Tamara Kovalenko, Vlad Polataev, Gerilyn Soreghan, Neil Tabor, and, in particular, John Isbell.

LITERATURE CITED

Algeo TJ, Heckel PH. 2008. The Late Pennsylvanian midcontinent sea of North America: a review. *Palaeogeogr. Palaeoclimatol. Palaeoecol.* 268:205–21

Allen JP, Fielding CR, Gibling MR, Rygel MC. 2011. Fluvial response to paleo-equatorial climate fluctuations during the late Paleozoic ice age. *Geol. Soc. Am. Bull.* 123:1524–38

Angiolini L, Gaetani M, Muttoni G, Stephenson MH, Zanchi A. 2007. Tethyan oceanic currents and climate gradients 300 m.y. ago. *Geology* 35:1071–74

Angiolini L, Jadoul F, Leng MJ, Stephenson MH, Rushton J, et al. 2009. How cold were the early Permian glacial tropics? Testing sea-surface temperature using the oxygen isotope composition of rigorously screened brachiopod shells. *J. Geol. Soc. Lond.* 166:933–45

Ballantyne AP, Levine M, Crowley TJ, Liu J, Baker PB. 2005. Meta-analysis of tropical surface temperatures during the Last Glacial Maximum. *Geophys. Res. Lett.* 32:L05712

Bates SM, Lyons TW, Montañez IP, Poulsen CJ, Horton DE. 2011. *Coupled conodont $\delta^{18}O$ phosphate, climate model, and stratigraphic perspectives on Carboniferous cyclic deposits from mid-Continent North America*. Presented at Am. Geophys. Union Fall Meet., Dec. 5–9, San Francisco

Berner RA. 2006. GEOCARBSULF: a combined model for Phanerozoic atmospheric O_2 and CO. *Geochim. Cosmochim. Acta* 70:5653–64

Best ES, Heckel PH, Lentz LJ, Bragonier WA, Lyons TW. 2011. Record of glacial-eustatic sea-level fluctuations in complex Middle to Late Pennsylvanian facies in the Northern Appalachian Basin and relation to similar events in the Midcontinent basin. *Sediment. Geol.* 238:79–100

Birgenheier LP, Fielding CR, Rygel MC, Frank TD, Roberts J. 2009. Evidence for dynamic climate change on sub-10^6-year scales from the late Paleozoic glacial record, Tamworth Belt, New South Wales, Australia. *J. Sediment. Res.* 79:56–82

Birgenheier LP, Frank TD, Fielding CR, Rygel MC. 2010. Coupled carbon isotopic and sedimentological records from the Permian system of eastern Australia reveal the response of atmospheric carbon dioxide to glacial growth and decay during the late Palaeozoic Ice Age. *Palaeogeogr. Palaeoclimatol. Palaeoecol.* 286:178–93

Bishop JW, Montañez IP, Gulbranson EL, Brenckle PL. 2009. The onset of mid-Carboniferous glacio-eustasy: sedimentologic and diagenetic constraints, Arrow Canyon, Nevada. *Palaeogeogr. Palaeoclimatol. Palaeoecol.* 276:217–43

Bishop JW, Montañez IP, Osleger DA. 2010. Dynamic Carboniferous climate change, Arrow Canyon, Nevada. *Geosphere* 6:1–34

Blake BM, Beuthin JD. 2008. Deciphering the mid-Carboniferous eustatic event in the central Appalachian foreland basin, southern West Virginia, USA. See Fielding et al. 2008c, pp. 249–60

Blakey RC. 2008. Gondwana paleogeography from assembly to breakup—a 500 m.y. odyssey. See Fielding et al. 2008c, pp. 1–28

Brandley RT, Krause FF. 1997. Upwelling, thermoclines and wave-sweeping on an equatorial carbonate ramp: lower carboniferous strata of western Canada. *Soc. Sediment. Geol. Spec. Publ.* 56:365–90

Brezinski DK, Cecil CB, Skema VW, Stamm R. 2008. Late Devonian glacial deposits from the eastern United States signal an end of the mid-Paleozoic warm period. *Palaeogeogr. Palaeoclimatol. Palaeoecol.* 268:143–51

Buggisch W, Joachimski MM, Sevastopulo G, Morrow JR. 2008. Mississippian $\delta^{13}C$ (carb) and conodont apatite $\delta^{18}O$ records—their relation to the late Palaeozoic Glaciation. *Palaeogeogr. Palaeoclimatol. Palaeoecol.* 268:273–92

Caputo MV, Goncalves de Melo JH, Streel M, Isbell JL. 2008. Late Devonian and early Carboniferous glacial records of South America. See Fielding et al. 2008c, pp. 161–74

Cecil BC, Dulong FT, West RR, Stamm R, Wardlaw B, Edgar NT. 2003. Climate controls on the stratigraphy of a Middle Pennsylvanian cyclothem in North America. *Soc. Sediment. Geol. Spec. Publ.* 77:151–82

Clapham ME. 2010. Faunal evidence for a cool boundary current and decoupled regional climate cooling in the Permian of western Laurentia. *Palaeogeogr. Palaeoclimatol. Palaeoecol.* 298:348–59

Clapham ME, James NP. 2008. Paleoecology of early-middle Permian marine communities in eastern Australia: response to global climate change in the aftermath of the late Paleozoic ice age. *PALAIOS* 23:738–50

Cleal C, James RM, Zodrow EL. 1999. Variation in stomatal density in the late Carboniferous gymnosperm from *Neuropteris ovata*. *PALAIOS* 14:180–85

Cleal CJ, Thomas BA. 2005. Palaeozoic tropical rainforests and their effect on global climates: Is the past the key to the present? *Geobiology* 3:13–31

Crowell JC. 1999. *Pre-Mesozoic Ice Ages: Their Bearing on Understanding the Climate System*. Geol. Soc. Am. Mem. 192. Boulder, CO: Geol. Soc. Am. 106 pp.

Crowley TJ, Baum SK. 1991. Estimating Carboniferous sea-level fluctuations from Gondwanan ice extent. *Geology* 19:975–77

Crowley TJ, Baum SK. 1992. Modeling late Paleozoic glaciation. *Geology* 20:507–10

Davydov VI, Korn D, Schmitz MD. 2012. The Carboniferous Period. In *The Geologic Time Scale 2012*, Vol. 1, ed. F Gradstein, J Ogg, M. Schmitz, G Ogg, pp. 615–63. Boston: Elsevier

Dickins JM. 1996. Problems of a late Palaeozoic glaciation in Australia and subsequent climate in the Permian. *Palaeogeogr. Palaeoclimatol. Palaeoecol.* 125:185–97

DiMichele WA, Montañez IP, Poulsen CJ, Tabor NJ. 2009. Climate and vegetational regime shifts in the late Paleozoic ice age earth. *Geobiology* 7:200–226

DiMichele WA, Pfefferkorn HW, Gastaldo RA. 2001. Response of late Carboniferous and early Permian plant communities to climate change. *Annu. Rev. Earth Planet. Sci.* 29:461–87

Durante M. 2000. Global cooling in the middle Carboniferous. *Newsl. Carbonif. Stratigr.* 18:31–32

Elrick M, Scott LA. 2010. Carbon and oxygen isotope evidence for high-frequency (104–105 yr) and My-scale glacio-eustasy in Middle Pennsylvanian cyclic carbonates (Gray Mesa Formation), central New Mexico. *Palaeogeogr. Palaeoclimatol. Palaeoecol.* 285:307–20

Epshteyn OG. 1981. Middle Carboniferous ice-marine deposits of northeastern U.S.S.R. In *Earth's Pre-Pleistocene Glacial Record*, ed. MJ Hambrey, WB Harland, pp. 268–69. Cambridge, UK: Cambridge Univ. Press

Eros JM, Montañez IP, Davydov VI, Osleger DA, Nemyrovska TI, et al. 2012a. Reply to the comment on "Sequence stratigraphy and onlap history of the Donets Basin, Ukraine: insight into Carboniferous icehouse dynamics." *Palaeogeogr. Palaeoclimatol. Palaeoecol.* 363–364:187–91

Eros JM, Montañez IP, Osleger DA, Davydov VI, Nemyrovska T, et al. 2012b. Sequence stratigraphy and onlap history of the Donets Basin, Ukraine: insight into Carboniferous icehouse dynamics. *Palaeogeogr. Palaeoclimatol. Palaeoecol.* 313–314:1–25

Eyles N. 1993. Earth's glacial record and its tectonic setting. *Earth-Sci. Rev.* 35:1–248

Falcon-Lang HJ, DiMichele WA. 2010. What happened to the coal forests during Pennsylvanian glacial phases? *PALAIOS* 25:611–17

Falcon-Lang HJ, Heckel PH, DiMichele WA, Blake BM Jr, Easterday CR, et al. 2011. No major stratigraphic gap exists near the Middle-Upper Pennsylvanian (Desmoinesian-Missourian) boundary in North America. *PALAIOS* 26:125–39

Feldman HR, Franseen EK, Joeckel RM, Heckel PH. 2005. Impact of longer-term modest climate shifts on architecture of high-frequency sequences (cyclothems), Pennsylvanian of Midcontinent U.S.A. *J. Sediment. Res.* 75:360–68

Fielding CR, Frank TD, Birgenheier LP, Rygel MC, Jones AT, Roberts J. 2008a. Stratigraphic imprint of the Late Palaeozoic Ice Age in eastern Australia: a record of alternating glacial and non-glacial climate regime. *J. Geol. Soc. Lond.* 165:129–40

Fielding CR, Frank TD, Birgenheier LP, Rygel MC, Jones AT, Roberts J. 2008b. Stratigraphic record and facies associations of the late Paleozoic ice age in eastern Australia (New South Wales and Queensland). See Fielding et al. 2008c, pp. 41–58

Fielding CR, Frank TD, Isbell JL, eds. 2008c. *Resolving the Late Paleozoic Ice Age in Time and Space*. Geol. Soc. Am. Spec. Publ. 441. Boulder, CO: Geol. Soc. Am. 354 pp.

Fielding CR, Frank TD, Isbell JL. 2008d. The late Paleozoic ice age—a review of current understanding and synthesis of global climate patterns. See Fielding et al. 2008c, pp. 343–54

Fielding CR, Frank TD, Isbell JL, Henry LC, Domack EW. 2010. Stratigraphic signature of the late Paleozoic Ice Age in the Parmeener Supergroup of Tasmania, SE Australia, and inter-regional comparisons. *Palaeogeogr. Palaeoclimatol. Palaeoecol.* 298:79–90

Fischbein SA, Joeckel RM, Fielding CR. 2009. Fluvial-estuarine reinterpretation of large, isolated sandstone bodies in epicontinental cyclothems, Upper Pennsylvanian, northern Midcontinent, USA, and their significance for understanding late Paleozoic sea-level fluctuations. *Sediment. Geol.* 216:15–28

Frakes LA, Francis JE. 1988. A guide to Phanerozoic cold polar climates from high-latitude ice-rafting in the Cretaceous. *Nature* 333:547–49

Frakes LA, Francis JE, Syktus JI. 1992. *Climate Modes of the Phanerozoic*. Cambridge, UK: Cambridge Univ. Press

Frank TD, Birgenheier LP, Montañez IP, Fielding CR, Rygel MC. 2008. Late Paleozoic climate dynamics revealed by comparison of ice-proximal stratigraphic and ice-distal isotopic records. See Fielding et al. 2008c, pp. 331–42

Gastaldo RA, DiMichele WA, Pfefferkorn HW. 1996. Out of the icehouse into the greenhouse: a late Paleozoic analog for modern global vegetational change. *GSA Today* 6:1–7

Giles PS. 2012. Low-latitude Ordovician to Triassic brachiopod habitat temperatures (BHTs) determined from $\delta^{18}O_{[\text{brachiopod calcite}]}$: a cold hard look at ice-house tropical oceans. *Palaeogeogr. Palaeoclimatol. Palaeoecol.* 317–18:134–52

González CR. 1990. Development of the late Paleozoic glaciations of the South American Gondwana in western Argentina. *Palaeogeogr. Palaeoclimatol. Palaeoecol.* 79:275–87

González CR. 2001. New data on the late Palaeozoic glaciations in Argentina. *Newsl. Carbonif. Stratigr.* 19:44–45

González CR, Díaz Saravia P. 2010. Bimodal character of late Paleozoic glaciations in Argentina and bipolarity of climatic changes. *Palaeogeogr. Palaeoclimatol. Palaeoecol.* 298:101–11

Grossman EL, Yancey TE, Jones TE, Chuvashov B, Mazzullo SJ, Mii H-S. 2008. Glaciation, aridification, and carbon sequestration in the Permo-Carboniferous: the isotopic record for low latitudes. *Palaeogeogr. Palaeoclimatol. Palaeoecol.* 268:222–33

Gulbranson EL, Montañez IP, Schmitz MD, Limarino CO, Isbell JL, et al. 2010. High-precision U-Pb calibration of Carboniferous glaciation and climate history, NW Argentina. *Geol. Soc. Am. Bull.* 122:1480–98

Haug GH, Tiedemann R. 1998. Effect of the formation of the Isthmus of Panama on Atlantic Ocean thermohaline circulation. *Nature* 393:673–76

Heckel PH. 1977. Origin of phosphatic black shale facies in Pennsylvanian cyclothems of mid-continent North America. *AAPG Bull.* 61:1045–68

Heckel PH. 1986. Sea-level curve for Pennsylvanian eustatic marine transgressive-regressive cycles along midcontinent outcrop belt, North America. *Geology* 14:330–34

Heckel PH. 1994. Evaluation of evidence for glacio-eustatic control over marine Pennsylvanian cyclothems in North America and consideration of possible tectonic effects. In *Concepts in Sedimentology and Paleontology*, Vol. 4: *Tectonic and Eustatic Controls on Sedimentary Cycles*, ed. JM Dennison, FR Ettensohn, pp. 65–87. Tulsa, OK: Soc. Sediment. Geol.

Henderson CM, Davydov VI, Wardlaw BR. 2012. The Permian Period. In *The Geologic Time Scale 2012*, Vol. 1, ed. F Gradstein, J Ogg, M Schmitz, G Ogg, pp. 665–93. Boston: Elsevier

Henry LC, Isbell JL, Limarino CO. 2008. Carboniferous glacigenic deposits of the proto-Precordillera of west-central Argentina. See Fielding et al. 2008c, pp. 131–42

Henry LC, Isbell JL, Limarino CO, McHenry LJ, Fraiser ML. 2010. Mid-Carboniferous deglaciation of the Protoprecordillera, Argentina, recorded in the Agua de Jagüel paleovalley. *Palaeogeogr. Palaeoclimatol. Palaeoecol.* 298:112–29

Herrington A, Poulsen CJ. 2012. Terminating the last interglacial: the role of ice sheet–climate feedbacks in a GCM asynchronously coupled to an ice sheet model. *J. Clim.* 25:1871–82

Holz M, Franca AB, Souza PA, Iannuzzi R, Rohn R. 2010. A stratigraphic chart of the Late Carboniferous/Permian succession of the eastern border of the Parana Basin, Brazil, South America. *J. S. Am. Earth Sci.* 29:381–99

Horton DE, Poulsen CJ. 2009. Paradox of late Paleozoic glacioeustasy. *Geology* 37:715–18

Horton DE, Poulsen CJ, Montañez IP, DiMichele WA. 2012. Eccentricity-paced late Paleozoic climate change. *Palaeogeogr. Palaeoclimatol. Palaeoecol.* 331–32:150–61

Horton DE, Poulsen CJ, Pollard D. 2007. Orbital and CO_2 forcing of late Paleozoic continental ice sheets. *Geophys. Res. Lett.* 34:L19708

Horton DE, Poulsen CJ, Pollard D. 2010. Influence of high-latitude vegetation feedbacks on late Paleozoic glacial cycles. *Nat. Geosci.* 3:572–77

Hughes TJ, Denton GH, Andersen BG, Schilling DH, Fastook JL, Lingle CS. 1981. The last great ice sheets: a global view. In *The Last Great Ice Sheets*, ed. GH Denton, TJ Hughes, pp. 263–317. New York: Wiley. 484 pp.

Hyde WT, Crowley TJ, Tarasov L, Peltier WR. 1999. The Pangean ice age: studies with a coupled climate-ice sheet model. *Clim. Dyn.* 15:619–29

Hyde WT, Grossman EL, Crowley TJ, Pollard D, Scotese CR. 2006. Siberian glaciation as a constraint on Permian–Carboniferous CO_2 levels. *Geology* 34:421–24

Iannuzzi R, Pfefferkorn HW. 2002. A pre-glacial, warm-temperature floral belt in Gondwana (late Visean, early Carboniferous). *PALAIOS* 17:571–90

Isaacson PE, Diaz-Martinez E, Grader GW, Kalvoda J, Babek O, Devuyst FX. 2008. Late Devonian–earliest Mississippian glaciation in Gondwanaland and its biogeographic consequences. *Palaeogeogr. Palaeoclimatol. Palaeoecol.* 268:126–42

Isbell JL, Cole DI, Catuneanu O. 2008a. Carboniferous-Permian glaciation in the main Karoo Basin, South Africa: stratigraphy depositional controls, and glacial dynamics. See Fielding et al. 2008c, pp. 71–82

Isbell JL, Henry LC, Gulbranson EL, Limarino CO, Fraiser ML, et al. 2012. Glacial paradoxes during the late Paleozoic ice age: evaluating the equilibrium line altitude as a control on glaciation. *Gondwana Res.* 22:1–19

Isbell JL, Koch ZJ, Szablewski GM, Lenaker PA. 2008b. Permian glacigenic deposits in the Transantarctic Mountains, Antarctica. See Fielding et al. 2008c, pp. 59–70

Isbell JL, Miller MF, Wolfe KL, Lenaker PA. 2003. Timing of late Paleozoic glaciation in Gondwana: Was glaciation responsible for the development of Northern Hemisphere cyclothems? *Geol. Soc. Am. Spec. Publ.* 370:5–24

Jacobs DK, Sahagian DL. 1993. Climate-induced fluctuations in sea-level during non-glacial times. *Nature* 361:710–12

Joachimski MM, von Bitter PH, Buggisch W. 2006. Constraints on Pennsylvanian glacio-eustatic sea-level changes using oxygen isotopes on conodont apatite. *Geology* 34:277–80

Jones AT, Frank TD, Fielding CR. 2006. Cold climate in the eastern Australian mid to late Permian may reflect cold upwelling waters. *Palaeogeogr. Palaeoclimatol. Palaeoecol.* 237:370–77

Kabanov PB, Alekseeva TV, Alekseeva VA, Alekseev AO, Gubin SV. 2010. Paleosols in late Moscovian (Carboniferous) marine carbonates of the East European Craton revealing "Great Calcimagnesian Plain" paleolandscapes. *J. Sediment. Res.* 80:195–215

Kammer TW, Matchen DL. 2008. Evidence for eustasy at the Kinderhookian-Osagean (Mississippian) boundary in the United States: response to late Tournaisian glaciation? See Fielding et al. 2008c, pp. 261–74

Kiehl JT, Shields CA. 2005. Climate simulation of the latest Permian: implications for mass extinction. *Geology* 33:757–60

Klocker A, Prange M, Schulz M. 2005. Testing the influence of the Central American Seaway on orbitally forced Northern Hemisphere glaciation. *Geophys. Res. Lett.* 32:L03703

Koch JT, Frank TD. 2011. The Pennsylvanian–Permian transition in the low-latitude carbonate record and the onset of major Gondwanan glaciation. *Palaeogeogr. Palaeoclimatol. Palaeoecol.* 308:362–72

Korte C, Jones PJ, Brand U, Mertmann D, Veizer J. 2008. Oxygen isotope values from high-latitudes: clues for Permian sea-surface temperature gradients and late Paleozoic deglaciation. *Palaeogeogr. Palaeoclimatol. Palaeoecol.* 269:1–16

Kutzbach JE, Gallimore RG. 1989. Pangaean climates: megamonsoons of the megacontinent. *J. Geophys. Res. Atmos.* 94:3341–57

Kutzbach JE, Guetter PJ. 1990. Simulated circulation of an idealized ocean for Pangaean time. *Paleoceanography* 5:299–317

Lee S-Y, Poulsen CJ. 2006. Sea ice control on Plio-Pleistocene evolution of the tropical Pacific climate. *Earth Planet. Sci. Lett.* 248:253–62

Limarino C, Tripaldi A, Marenssi S, Fauqué L. 2006. Tectonic, sea-level, and climatic controls on late Paleozoic sedimentation in the western basins of Argentina. *J. S. Am. Earth Sci.* 22:205–26

Lopez-Gamundi OR, Buatois LA, eds. 2010. *Late Paleozoic Glacial Events and Postglacial Transgressions in Gondwana*. Geol. Soc. Am. Spec. Publ. 468. Boulder, CO: Geol. Soc. Am. 207 pp.

Martin JR, Redfern J, Aitken JF. 2008. A regional overview of the late Paleozoic glaciation in Oman. See Fielding et al. 2008c, pp. 175–86

Martin L, Montañez IP, Bishop J. 2012. Carboniferous sequence stratigraphy and sea-level history of the Bird Spring Platform, Southern Great Basin, USA. *Palaeogeogr. Palaeoclimatol. Palaeoecol.* 329:64–82

McGhee GR Jr, Sheehan PM, Bottjer DJ, Droser ML. 2012. Ecological ranking of Phanerozoic biodiversity crises: The Serpukhovian (early Carboniferous) crisis had a greater ecological impact than the end-Ordovician. *Geology* 40:147–50

Mii HS, Grossman DS, Yancey TE, Chuvashov B, Egorov A. 2001. Isotopic records of brachiopod shells from the Russian Platform—evidence for the onset of mid-Carboniferous glaciation. *Chem. Geol.* 175:133–47

Mii HS, Shi GR, Cheng C-J, Chen Y-Y. 2012. Permian Gondwanaland paleoenvironment inferred from carbon and oxygen isotope records of brachiopod fossils from Sydney Basin, southeast Australia. *Chem. Geol.* 291:87–103

Miller KB, McCahon TJ, West RR. 1996. Lower Permian (Wolfcampian) paleosol-bearing cycles of the U.S. midcontinent: evidence of climatic cyclicity. *J. Sediment. Res.* 66:71–84

Montañez IP, Norris RD, Algeo T, Chandler MA, Johnson KR, et al. 2011. *Understanding Earth's Deep Past: Lessons for Our Climate Future.* Washington, DC: Natl. Acad. Press. 161 pp.

Montañez IP, Tabor NJ, Niemeier D, DiMichele WA, Frank TD, et al. 2007. CO_2-forced climate instability and linkages to tropical vegetation during late Paleozoic deglaciation. *Science* 315:87–91

Mory AJ, Redfern J, Martin JR. 2008. A review of Permian-Carboniferous glacial deposits in Western Australia. See Fielding et al. 2008c, pp. 29–40

Olszewski TD, Patzkowsky ME. 2008. Icehouse climate and eustasy recorded on a low-latitude epeiric platform: alternating climate regimes in the Pennsylvanian-Permian succession of the North American midcontinent. *Geol. Assoc. Can. Spec. Pap.* 48:1–17

Otto-Bliesner B. 1996. Initiation of a continental ice sheet in a global climate model (GENESIS). *J. Geophys. Res.* 101(D12):16909–20

Pérez Loinaze VS, Limarino CO, Césari SN. 2010. Glacial events in Carboniferous sequences from Paganzo and Río Blanco Basins (Northwest Argentina): palynology and depositional setting. *Geol. Acta* 8:399–418

Perlmutter MA, Matthews MD. 1989. Global cyclostratigraphy: a model. In *Quantitative Dynamic Stratigraphy*, ed. TA Cross, pp. 233–60. Amsterdam: Elsevier

Peters SE. 2007. The problem with the Paleozoic. *Paleobiology* 33:165–81

Peyser CE, Poulsen CJ. 2008. Controls on Permo-Carboniferous precipitation over tropical Pangea: a GCM sensitivity study. *Palaeogeogr. Palaeoclimatol. Palaeoecol.* 268:181–92

Poulsen CJ, Pollard D, Montañez IP, Rowley D. 2007. Late Paleozoic tropical climate response to Gondwanan deglaciation. *Geology* 35:771–74

Powell MG. 2005. Climatic basis for sluggish macroevolution during the late Palaeozoic ice age. *Geology* 33:381–84

Powell MG. 2007. Latitudinal diversity gradients for brachiopod genera during late Palaeozoic time: links between climate, biogeography and evolutionary rates. *Glob. Ecol. Biogeogr.* 16:519–28

Powell MG, Schöne BR, Dorrit EJ. 2009. Tropical marine climate during the late Paleozoic ice age using trace element analysis of brachiopods. *Palaeogeogr. Palaeoclimatol. Palaeoecol.* 280:143–49

Rankey EC. 1997. Relations between relative changes in sea level and climate shifts: Pennsylvanian-Permian mixed carbonate-siliciclastic strata, western United States. *Geol. Soc. Am. Bull.* 109:1089–100

Raymond A, Metz C. 2004. Ice and its consequences: glaciation in the Late Ordovician, Late Devonian, Pennsylvanian-Permian, and Cenozoic compared. *J. Geol.* 112:655–70

Reid CM, James NP, Beauchamp B, Kyser TK. 2007. Faunal turnover and changing oceanography: late Palaeozoic warm-to-cool water carbonates, Sverdrup Basin, Canadian Arctic Archipelago. *Palaeogeogr. Palaeoclimatol. Palaeoecol.* 249:128–59

Rocha-Campos AC, dos Santos PR, Canuto JR. 2008. Late Paleozoic glacial deposits of Brazil: Parana Basin. See Fielding et al. 2008c, pp. 97–114

Roe GH, Lindzen RS. 2001. The mutual interaction between continental-scale ice sheets and atmospheric stationary waves. *J. Clim.* 14:1450–65

Roscher M, Schneider JW. 2006. Permo-Carboniferous climate: Early Pennsylvanian to late Permian climate development of Central Europe in a regional and global context. *Geol. Soc. Lond. Spec. Publ.* 265:95–136

Ross CA, Ross JRP. 1987. Late Paleozoic sea levels and depositional sequences. *Cushman Found. Foraminifer. Res. Spec. Publ.* 24:137–49

Rygel MC, Fielding CR, Frank TD, Birgenheier LP. 2008. The magnitude of late Paleozoic glacioeustatic fluctuations: a synthesis. *J. Sediment. Res.* 78:500–11

Saltzman MR. 2002. Carbon and oxygen isotope stratigraphy of the Lower Mississippian (Kinderhookian–lower Osagean), western United States: implications for seawater chemistry and glaciation. *Geol. Soc. Am. Bull.* 114:96–108

Saltzman MR. 2003. Late Paleozoic ice age: oceanic gateway or $p\mathrm{CO_2}$? *Geology* 31:151–54

Shi GR, Chen ZQ. 2006. Lower Permian oncolites from South China: implications for equatorial sea-level responses to late Palaeozoic Gondwanan glaciation. *J. Asian Earth Sci.* 26:424–36

Shi GR, Waterhouse JB. 2010. Late Palaeozoic global changes affecting high-latitude environments and biotas: an introduction. *Palaeogeogr. Palaeoclimatol. Palaeoecol.* 298:1–16

Smith LB Jr, Read JF. 2000. Rapid onset of late Paleozoic glaciation on Gondwana: evidence from Upper Mississippian strata of the midcontinent, United States. *Geology* 28:279–82

Soreghan GS. 1994. The impact of glacioclimatic change on Pennsylvanian cyclostratigraphy. *Can. Soc. Pet. Geol. Mem.* 17:523–43

Soreghan GS, Elmore RD, Lewchuk MT. 2002. Sedimentological record of western Pangean climate in upper Paleozoic loessite. *Geol. Soc. Am. Bull.* 114:1019–35

Soreghan GS, Soreghan MJ, Poulsen CJ, Young RA, Eble CF, et al. 2008. Anomalous cold in the Pangaean tropics. *Geology* 36:659–62

Soreghan MJ, Soreghan GS, Hamilton MA. 2008. Glacial-interglacial shifts in atmospheric circulation of western tropical Pangaea. *Palaeogeogr. Palaeoclimatol. Palaeoecol.* 268:260–72

Stanley S, Powell MG. 2003. Depressed rates of origination and extinction during the late Paleozoic ice age: a new state for the global marine ecosystem. *Geology* 31:877–80

Stemmerick L. 2008. Influence of late Paleozoic Gondwana glaciations on the depositional evolution of the northern Pangean shelf, North Greenland, Svalbard, and the Barents Sea. See Fielding et al. 2008c, pp. 205–18

Stollhofen H, Werner M, Stanistreet IG, Armstrong RA. 2008. Single-zircon U-Pb dating of Carboniferous-Permian tuffs, Namibia, and the intercontinental deglaciation cycle framework. See Fielding et al. 2008c, pp. 83–96

Taboada AC. 2010. Mississippian–early Permian brachiopods from western Argentina: tools for middle- to high-latitude correlation, paleobiogeographic and paleoclimatic reconstruction. *Palaeogeogr. Palaeoclimatol. Palaeoecol.* 298:152–75

Tabor NJ, Montañez IP, Scotese CR, Poulsen CJ, Mack GH. 2008. Paleosol archives of environmental and climatic history in paleotropical western Pangea during the latest Pennsylvanian through early Permian. See Fielding et al. 2008c, pp. 291–304

Tabor NJ, Poulsen CJ. 2008. Late Paleozoic tropical climate and atmospheric circulation: a review of paleoclimate indicators and models. *Palaeogeogr. Palaeoclimatol. Palaeoecol.* 268:181–92

Tandon SK, Gibling MR. 1994. Calcrete and coal in Late Carboniferous cyclothems of Nova Scotia, Canada: climate and sea-level changes linked. *Geology* 22:755–58

Veevers JJ, Powell CM. 1987. Late Paleozoic glacial episodes in Gondwanaland reflected in transgressive-regressive depositional sequences in Euramerica. *Geol. Soc. Am. Bull.* 98:475–87

Visser JNJ. 1997. A review of the Permo-Carboniferous glaciation in Africa. In *Late Glacial and Postglacial Environmental Changes: Quaternary, Carboniferous-Permian, and Proterozoic*, ed. IP Martini, pp. 169–91. New York: Oxford Univ. Press

Wanless HR, Shepard FP. 1936. Sea level and climate changes related to late Paleozoic cycles. *Geol. Soc. Am. Bull.* 47:1177–206

Waterhouse JB, Shi GR. 2010. Evolution of a cold climate. *Palaeogeogr. Palaeoclimatol. Palaeoecol.* 298:17–30

Waters CN, Condon DJ. 2012. Nature and timing of Late Mississippian to Mid-Pennsylvanian glacio-eustatic sea-level changes of the Pennine Basin, UK. *J. Geol. Soc. Lond.* 169:37–51

West RR, Archer AW, Miller KB. 1997. The role of climate in stratigraphic patterns exhibited by late Palaeozoic rocks exposed in Kansas. *Palaeogeogr. Palaeoclimatol. Palaeoecol.* 128:1–16

Winguth AME, Heinze C, Kutzbach JE, Maier-Reimer E, Mikolajewicz U, et al. 2002. Simulated warm polar currents during the middle Permian. *Paleoceanography* 17:1057

Wopfner H, Casshyap SM. 1997. Transition from freezing to subtropical climates in the Permo-Carboniferous of Afro-Arabia and India. In *Late Glacial and Postglacial Environmental Changes: Quaternary, Carboniferous-Permian, and Proterozoic*, ed. IP Martini, pp. 192–212. New York: Oxford Univ. Press

Zhou J, Poulsen CJ, Pollard D, White TS. 2008. Simulation of modern and middle Cretaceous marine $\delta^{18}O$ with an ocean-atmosphere general circulation model. *Paleoceanography* 23:PA3223

Annual Review
of Earth and
Planetary Sciences

Volume 41, 2013

Contents